ARISTOTLE UNIVERSITY OF THESSALONIKI

Interinstitutional Program of Postgraduate Studies in
PALAEONTOLOGY – GEOBIOLOGY

MARIANNA KOKOTINI
Biologist

THE CERVIDAE (ARTIODACTYLA, MAMMALIA) FROM THE LOWER PLEISTOCENE FOSSIL SITE OF TSIOTRA VRYSSI (MYGDONIA BASIN)

MASTER THESIS

DIRECTION: Macropalaeontology. Directed by: Aristotle University of Thessaloniki

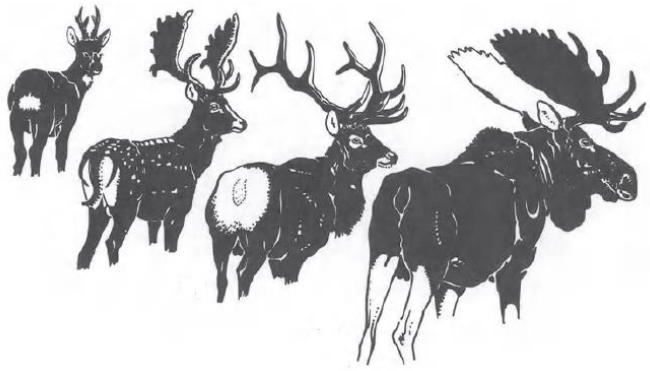

THESSALONIKI/ATHENS/PATRAS/MYTILINI

2020

Interinstitutional Program of Postgraduate Studies in

PALAEONTOLOGY – GEOBIOLOGY

supported by:

Τμήμα Γεωλογίας ΑΠΘ
School of Geology AUTh

Τμήμα Βιολογίας ΑΠΘ
School of Biology AUTh

National and Kapodistrian University of Athens
Faculty of Geology and Geoenvironment

Τμήμα Γεωλογίας & Γεωπεριβάλλοντος ΕΚΠΑ

Faculty of Geology & Geoenvironment NKUA

Department of GEOLOGY

Τμήμα Γεωλογίας Παν/μίου Πατρών
School of Geology, Patras Univ.

UNIVERSITY OF THE AEGEAN

Τμήμα Γεωγραφίας Παν/μίου Αιγαίου
Department of Geography, Aegean Univ.

MARIANNA ΚΟΚΟΤΙΝΙ
ΜΑΡΙΑΝΝΑ ΚΟΚΟΤΙΝΗ
Πτυχιούχος Βιολόγος

THE CERVIDAE (ARTIODACTYLA, MAMMALIA) FROM THE LOWER PLEISTOCENE FOSSIL SITE OF TSIOTRA VRYSSI (MYGDONIA BASIN)

ΤΑ ΕΛΑΦΟΕΙΔΗ ΤΗΣ ΚΑΤΩ-ΠΛΕΙΣΤΟΚΑΙΝΙΚΗΣ ΑΠΟΛΙΘΩΜΑΤΟΦΟΡΟΥ ΘΕΣΗΣ ΤΣΙΟΤΡΑ ΒΡΥΣΗ (ΛΕΚΑΝΗ ΜΥΓΔΟΝΙΑΣ)

Υποβλήθηκε στο ΔΠΜΣ Παλαιοντολογία-Γεωβιολογία

Ημερομηνία Προφορικής Εξέτασης: 17/03/2020
Oral Examination Date: 17/03/2020

Three-member Examining Board

Professor Dimitrios S. Kostopoulos, Supervisor
Professor Evangelia Tsoukala, Member
Professor Aikaterini Harvati-Papatheodorou, Member

Τριμελής Εξεταστική Επιτροπή

Καθηγητής Δημήτριος Κωστόπουλος, Επιβλέπων
Καθηγήτρια Ευαγγελία Τσουκαλά, Μέλος Τριμελούς Εξεταστικής Επιτροπής
Καθηγήτρια Αικατερίνη Χαρβάτη-Παπαθεοδώρου, Μέλος Τριμελούς Εξεταστικής Επιτροπής

External Assistant/Εξωτερικός Συνεργάτης (σύμφωνα με ΕΔΕ5/15-7-2019)
Dr. George E. Konidaris

THE CERVIDAE (ARTIODACTYLA, MAMMALIA) FROM THE LOWER PLEISTOCENE FOSSIL SITE OF TSIOTRA VRYSSI (MYGDONIA BASIN) – *Master Thesis*

ΤΑ ΕΛΑΦΟΕΙΔΗ ΤΗΣ ΚΑΤΩ-ΠΛΕΙΣΤΟΚΑΙΝΙΚΗΣ ΑΠΟΛΙΘΩΜΑΤΟΦΟΡΟΥ ΘΕΣΗΣ ΤΣΙΟΤΡΑ ΒΡΥΣΗ (ΛΕΚΑΝΗ ΜΥΓΔΟΝΙΑΣ) – *Μεταπτυχιακή Διπλωματική Εργασία*

Citation:
Kokotini Marianna., 2020. – The Cervidae (Artiodactyla, Mammalia) from the Lower Pleistocene fossil site of Tsiotra Vryssi (Mygdonia Basin). Master Thesis, Interinstitutional Program of Postgraduate Studies in Palaeontology-Geobiology. School of Geology, Aristotle University of Thessaloniki, 99 pp.

Cover Figure: Bubenik & Bubenik (1990)

Content

Acknowledgments

I am deeply thankful to Professor Dimitris Kostopoulos (Geology Department, Aristotle University of Thessaloniki), for assigning me the present MSc thesis and trusting me with the studied material. Dimitrios Kostopoulos embodies the standard of a teacher whose consultative role among the students aims at developing their scientific criteria, along with their very own viewpoints. Hereby, his notably constant guidance and support during the past months has been more than inspiring in terms of palaeontological research. I kindly thank Dr. George Konidaris for providing me information concerning the studied material, for the helpful recommendations on several bibliographic sources, along with his suggestions on the text. I also thank Professor Evangelia Tsoukala, and Professor Katerina Harvati-Papatheodorou, members of my examining board, for their suggestions concerning the text. To my fellow MSc students, Katerina Kafetzidou, Antipas Klitsas and Kostantis Laskos, I express my deep gratefulness for their invaluable companionship and support during the past year. To Dr. Ioannis Maniakas, MSc Nikos Kargopoulos and MSc Anastasia Gkeme, I express my appreciation for their friendly guidance. I also kindly thank Dr. Roman Croitor for the clarification of certain bibliographic sections. Finally, I most deeply thank my family for ceaselessly supporting me during both my undergraduate and postgraduate studies, and for entirely embracing my dedication to the field of palaeontology.

Abstract

The family Cervidae is generally regarded as one of the most abundant group of herbivores, including a considerable number of both extant and extinct species. The systematics of fossil deer has been particularly debatable through the years, due to the lack of complete fossil collections along with substantial taxonomic disagreements within the research community. In deer systematics, the morphology of antlers and dentition are considered as the most determining characters.

This work deals with the systematics of the cervids from the Lower Pleistocene fossiliferous site of Tsiotra Vryssi (TSR). TSR is located in Mygdonia Basin (Macedonia, Northern Greece) and after a series of systematic excavations, it has provided a plethora of fossil specimen, including several ones belonging to two deer species: a small-sized and a large-sized one. The faunal assemblage of the fossiliferous site of TSR is dated at 1.8-1.2 Ma.

The small-sized cervid is regarded as a new species of the genus *Cervus*, mainly due to its particularly distinct antler morphology, as compared to known Plio-Pleistocene European cervids of similar size. The large-sized cervid is attributed to *Praemegaceros* sp. Certain ecomorphological observations, concerning the habitat of the mentioned cervids, are pointed-out. Finally, certain Greek Villafranchian cervid faunal assemblages are also discussed, and compared to the one of Tsiotra Vryssi.

Περίληψη

Η οικογένεια των ελαφοειδών (Cervidae) θεωρείται ως μία από τις πιο ετερογενείς ομάδες φυτοφάγων θηλαστικών, καθώς περιλαμβάνει ένα υψηλό αριθμό, τόσο σύγχρονων όσο και απολιθωμένων μορφών. Το ζήτημα της συστηματικής των ελαφοειδών παραμένει ανοικτό, κυρίως λόγω της απουσίας επαρκούς απολιθωμένου υλικού, καθώς και της ύπαρξης ισχυρών διχογνωμιών ανάμεσα στην ερευνητική κοινότητα. Ως σημαντικότεροι χαρακτήρες στη συστηματική των Cervidae, κρίνονται οι μορφολογίες των κεράτων και των δοντιών.

Η παρούσα εργασία πραγματεύεται τη συστηματική των ελαφοειδών της Κατω-Πλειστοκαινικής απολιθωματοφόρου θέσης Τσιότρα Βρύση. Η θέση βρίσκεται στη Λεκάνη της Μυγδονίας (Μακεδονία) και ύστερα από μια σειρά συστηματικών ανασκαφών, απέδωσε σημαντικό αριθμό απολιθωμένου υλικού, συμπεριλαμβανομένων αυτών ενός μικρόσωμου και ενός μεγαλόσωμου ελαφοειδούς. Η πανιδική συνάθροιση της θέσης χρονολογείται περί τα 1.8-1.2 εκ. έτη πριν.

Ο μικρού μεγέθους αντιπρόσωπος της οικογένειας αποδίδεται σε νέο είδος του γένους *Cervus*, κυρίως λόγω της αρκετά διαφοροποιημένης μορφολογίας των κεράτων, σε σύγκριση με τα ως τώρα γνωστά παρομοίου μεγέθους Πλειο-Πλειστοκαινικά ελαφοειδή της Ευρώπης. Το μεγάλου μεγέθους ελαφοειδές αποδίδεται στο γένος *Praemegaceros*. Αναφέρονται ακόμη συγκεκριμένες οικομορφολογικές παρατηρήσεις που αφορούν τα ενδιαιτήματα των προαναφερθέντων ελαφοειδών. Τέλος, αναλύονται και συγκρίνονται επιλεγμένες συναθροίσεις ελαφοειδών Βιλλαφράγκιας ηλικίας του Ελλαδικού χώρου, με αυτή της Τσιότρα Βρύσης.

1. Introduction

1.1 The deer family

The Family Cervidae (Suborder Ruminantia), which is probably of Eurasiatic origin (Cap, 2002), includes a variety of approximately 40 extant species adapted in several different habitats. As a result, it is considered as one of the most diverse large-sized herbivore groups. The annually shed antlers and the absence of gallbladder, along with notable differences of chromosome numbers between relative forms, are distinctive characteristics of the deer (Cronin, 1991; Kuznetsova, 2005). Other main cranial characteristics (Fig. 1), such as the brachydont type of dentition and the presence of two lacrimal foramina, are also typical features (but not exclusive synapomorphies) of the family (Heckeberg, 2019).

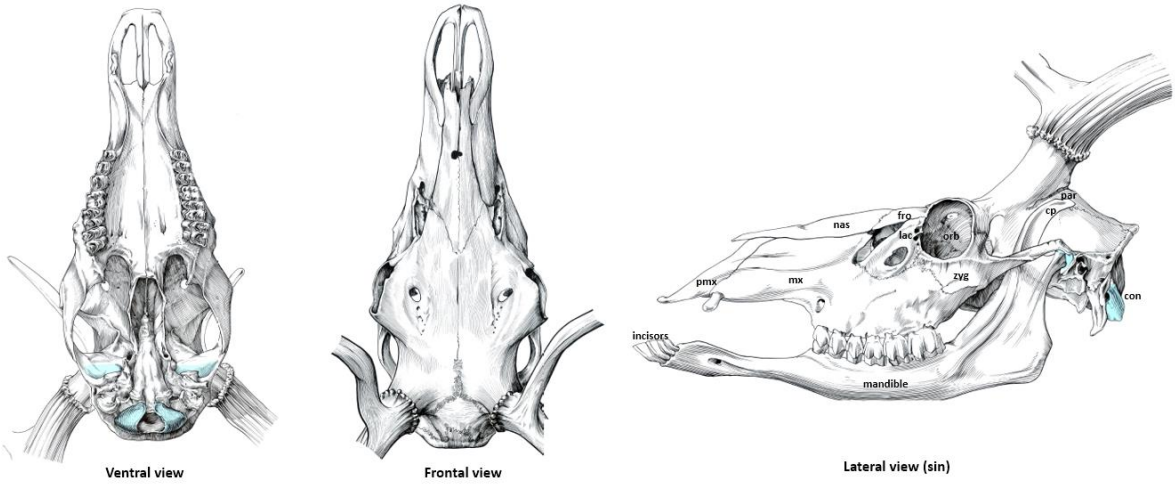

Figure 1. Skull of deer. Abbreviations: pmx = premaxillary, mx = maxillary, nas = nasal, lac = lacrimal, zyg = zygomaticum, orb = orbitosphenoid, fro = frontal, par = parietal, con = condyles, cp = coronoid process. Modified from Pales & Garcia (1971).

Concerning the relationships of the deer with the rest of the Ruminantia families, Kuznetsova (2005) based on genetic studies, showed that Cervidae and Bovidae are sister clades, with the latter being closer to musk deer (Moschidae). The monophyly of Cervidae, Bovidae and Moschidae is supported by several molecular studies (Hassanin et al., 2012; Yang, 2012).

Due to the richness of ecological forms, chaperoned by the fragmentary nature of the fossil deer record, the taxonomy of the cervids has been proved problematic over the years (Croitor, 2018). A first effort of classification was made by Brooke (1878), who divided the family into two large groups, based on the type of reduction of the second and fifth metacarpals: Plesiometacarpia (Subfamily Cervinae) and Telemetacarpia (Subfamilies Odocoileinae and Hydropotinae). Croitor (2018) summarized the classifications proposed by Lydekker (1898), Czyżewska (1968), Simpson (1945), Flerov (1952), Azzaroli (1953), Bouvrain et al. (1989), Vislobokova (1990) and Di Stefano & Petronio (2002), revealing at the same time persistent disagreements and controversial hypotheses concerning the taxonomy of certain genera, such as *Capreolus*, *Hydropotes* and elks (*Alces* and *Cervalces*). Molecular analysis by Gilbert (2006), has proved the dichotomy and monophyly of each of the two aforementioned groups and, as this study suggests, Plesiometacarpia includes the subfamilies Cervinae and Muntiacinae, whereas Telemetacarpalia include the subfamilies Odocoileinae and Hydropotinae.

Within the Pecoran family Gelocidae, which occurred in Eurasia in Eocene and included hornless ruminants, new forms under fast radiation originated during the Oligocene. (Cap, 2002), resulting to the extant families Antilocapridae, Giraffidae, Moschidae, Cervidae and Bovidae. The node of this clade can be traced between 32.0 and 28.1 Ma, and the diversification of the Cervidae subfamilies occurred during the the early Miocene. Some studies support that all the extant cervid subfamilies occurred at the interval between 25.4 and 13.5 Ma, with a major radiation event occuring between 20.2 and 16.9 Ma (Fernandez, 2005), whereas others place most of the current biodiversity of cervid tribes at the last 12 myr (Hassanin et al., 2012). The expansion of grasslands, the biogeographic land corridors between Africa and Eurasia, Eurasia and

North America, North America and South America, along with the radiation of large mammal predators (Hyaenidae, Felidae, Canidae), could explain the diversification of cervids and bovids at that time (Hassanin et al., 2012). The diversification of Plesiometacarpalia and Telemetacarpalia, occurred in the late Miocene. The advanced plesiometacarpal Old World cervids radiated from the Miocene/Pliocene boundary to the Early Pleistocene (Croitor, 2018).

According to Cap (2002), all male cervids of the early Miocene possessed upper canines, a characteristic identified as an ancestral trait (probably in order to dominate in their territory). During the Miocene, the upper canines became smaller, antlers appeared, and new locomotor adaptations evolved, related to open habitats (Curran, 2015). The appearance of antlers is connected to different social behaviors, and their enhanced size and complexity is an advanced character of the lineage (Geist, 1998). Concerning the dentition, within the plesiometacarpals the relatively short series of premolars along with a tendency of p4 molarization, are advanced trends of the Cervinae subfamily. The premolar/molar proportions of the plesiometacarpal deer are relatively stable, but in some of the most evolved genera (e.g., *Alces, Rangifer*) a most advanced molar-like p4 is observed. The molarization of lower premolars is an evolutionary trend, resulting to the increase of the grinding capability of the teeth, over the cutting one (Croitor, 2018).

1.2 Plio-Pleistocene cervids of Europe

As mentioned above, the phylogeny of the extinct deer is quite problematic due to the incompleteness of the fossil record. In this study, the systematics of the Plio-Pleistocene European deer proposed by Croitor (2018) will be followed. According to this scheme, the Subfamily Cervinae includes the following small to medium-sized genera: *Euprox* STEHLIN, 1928; *Metacervocerus* PORTIS, 1920; *Praeelaphus* PORTIS, 1920; *Dama* FRISCH, 1775; *Haploidoceros* CROITOR, BONIFAY & BRUGAL, 2008; as well as members of the genera *Cervus* LINNAEUS, 1758 and *Croizetoceros* HEINTZ, 1970. The large-sized Plio-Pleistocene cervids of Europe are assigned to the genera: *Arvernoceros* HEINTZ, 1920; *Eucladoceros* FALCONER 1868; *Praemegaceros* PORTIS, 1920; *Praedama*

PORTIS, 1920, as well as members of *Cervus*, *Megaloceros* BROOKES, 1828 and *Megaceroides* JOLEAUD, 1914.

The main diagnostic characters used in cervid systematics are related to the antler morphology (Fig. 2; Croitor, 2018). Apart from being well-preserved as fossil remains, antlers also provide ethological details of the studied species. In addition, antlers are indicative of sexual dimorphism and selection, creating great scientific interest in studying those patterns (Cronin, 1991). Nevertheless, antlers also show ontogenetic, pathologic or other kind of variations and as a result, the distiction of the genera should be sceptical in occasions (Heckeberg, 2019).

The antler characters used in a species level systematics are: the direction, shape and length of the antler beam; the number of tines; the development of palmation; the reduction of antler tines and the general simplification of antlers (Croitor, 2018).

The teeth morphology is also widely used in taxonomic analyses (Fig. 3). The main dental characters used in species level are: the development of the cingulum; the presence/absence of the *Palaeomeryx* fold and of other additional enamel folds; the premolar/molar ratio; and the degree of molarization of the lower fourth premolar (p4) (Croitor, 2018).

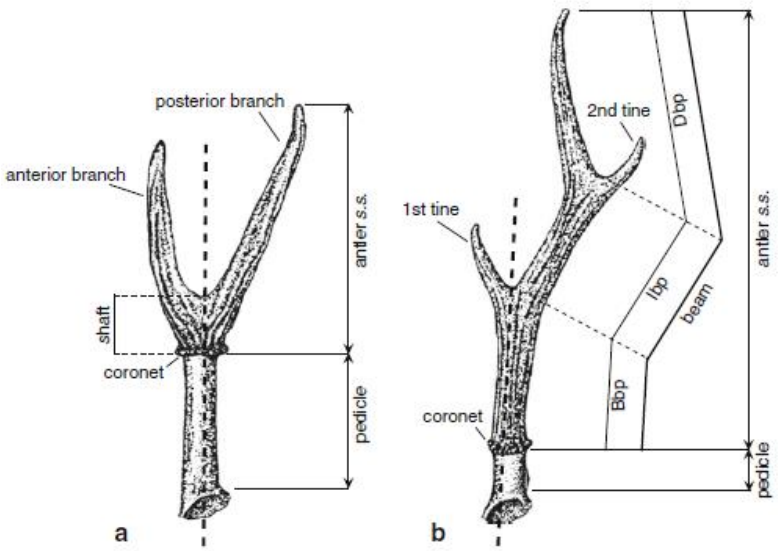

Figure 2. Main features of the cervid antler morphology. From Azanza et al. (2013).

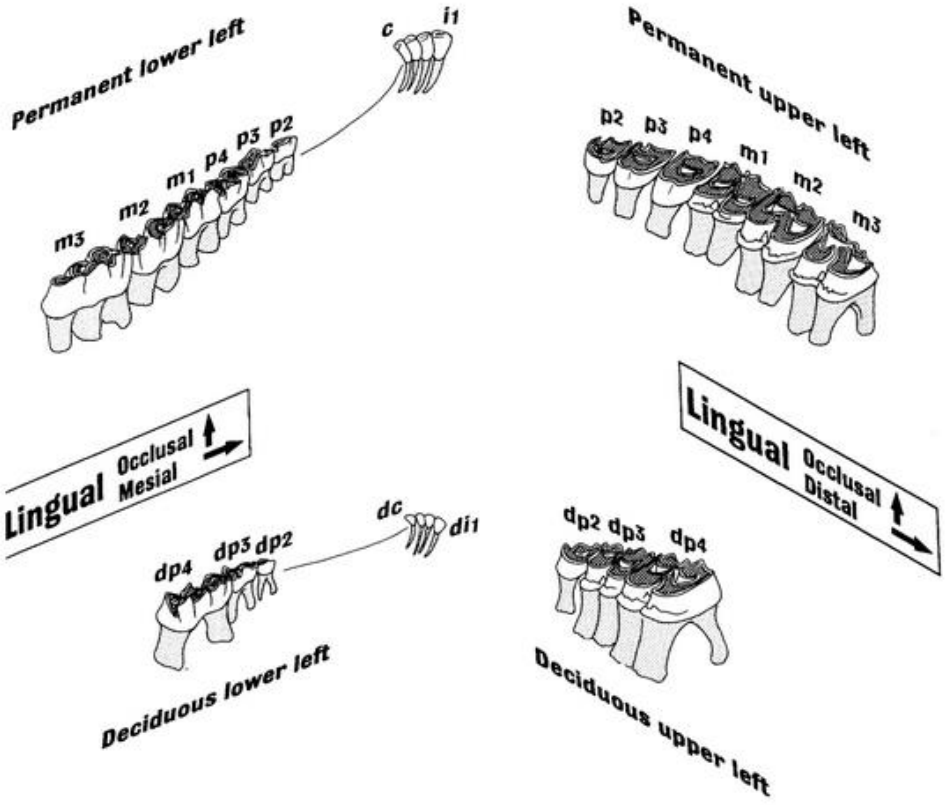

Figure 3. Dentition of deer. From Hillson (2016).

This study deals with the systematics of the cervids from the fossiliferous locality of Tsiotra Vryssi (Mygdonia Basin), and provides additionally some palaeoecological and biochronological remarks. The specimens will be metrically and morphologically compared with other known Plio-Pleistocene European deer, aiming to contribute to the taxonomy and evolution of the Early Pleistocene deer of Europe.

1.3 Geological setting and fossiliferous locality

Mygdonia basin. The Mydonia basin is located in Central Macedonia (Greece), to the northeast of Thessaloniki. Since the end of the 1970s, extensive fieldwork was carried

out by the Laboratory of Geology and Palaeontology of the Aristotle University of Thessaloniki (LGPUT) and led to the discovery of several fossiliferous sites that yielded a wealth of vertebrate fossils. Their systematic study, rendered Mygdonia basin as one of the European most significant regions in terms of studying, comparing and enriching the Pleistocene mammal fossil record.

The Mygdonia Basin is a large-scaled elongated east-west-trending tectonic depression. The beginning of its formation took place during the early-middle Miocene. The pre-Neogene central and eastern part of the basin consists of metamorphic rocks (schists, gneisses, amphibolites) of the Serbomacedonian Massif. The western part of the basin is formed by slightly metamorphosed sediments (phyllites, limestones, sandstones), which belong to the Circum-Rhodope Belt (Kockel et al., 1977).

The Pre-Mygdonia Basin (Fig. 4) was filled with fluvial-fluvioterrestrial and lacustrine sediments during the Neogene-Early Pleistocene. At the beginning of the Middle Pleistocene the N-S extensional tectonics in Northern Greece resulted into the division of the Pre-Mygdonia Basin into smaller subbasins (Psilovikos, 1977; Koufos et al., 1995), such as Mygdonia, Zagliveri, Doubia, and Marathoussa, which were filled mostly with lacustrine sediments. Psilovikos (1977) and later Koufos et al. (1995) separated the Neogene and Quaternary deposits of the basin in two main lithostratigraphic units: The Pre-Mygdonian Group and the Mygdonian Group. The former, consists of Neogene and Early Pleistocene deposits and includes three successive Formations: the Chryssavgi Fm, the Gerakarou Fm and the Platanochori Fm (Koufos et al., 1995).

Tsiotra Vryssi. The fossiliferous locality of Tsiotra Vryssi (TSR) was discovered in 2014 after systematic field survey in the Mygdonia basin. TSR is is geographically located in northern Chalkidiki, southwest of Krimni and north of Riza villages, and stratigraphically placed at the upper parts of the Gerakarou Formation.

The sediments of the locality consist of alternating beds of unconsolidated gravels, coarse sands, and reddish-brown silts and clays (Konidaris et al., 2015; Giusti et al., 2019; Fig. 5b).

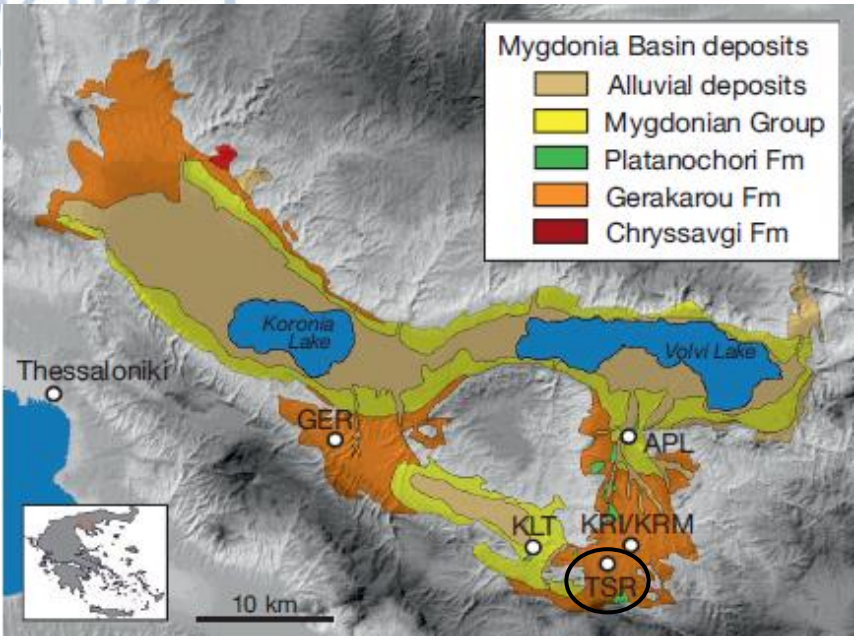

Figure 4. Geological map of the Neogene and Quaternary lithostratigraphic units of the Mygdonia Basin. The locality of TSR is indicated with a circle (map and data from Koufos et al., 1995; modified by Konidaris et al., 2015; Kostopoulos et al., 2018).

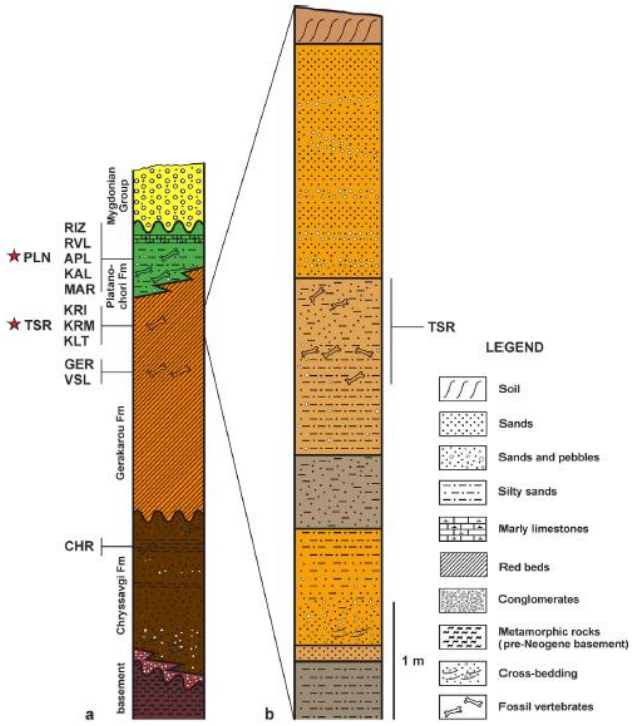

Figure 5. a: Simplified composite stratigraphic column of the Mygdonia Basin indicating the position of the old and new fossiliferous localities, data from Koufos et al., 1995; b: stratigraphic column of the Tsiotra Vryssi (TSR) locality (from Konidaris et al., 2015).

In 2014, surface findings along with exposed material were collected and the subsequent test excavation revealed a fossiliferous layer of vertebrate remains in the middle–upper part of the section. Systematic excavations are conducted from 2015 onwards, enriching substantially the TSR fossil collection. Some of the remains are anatomically connected (Fig. 6), but the majority of the fossils represent isolated specimens. The preliminary faunal list for TSR is given in Table 1.

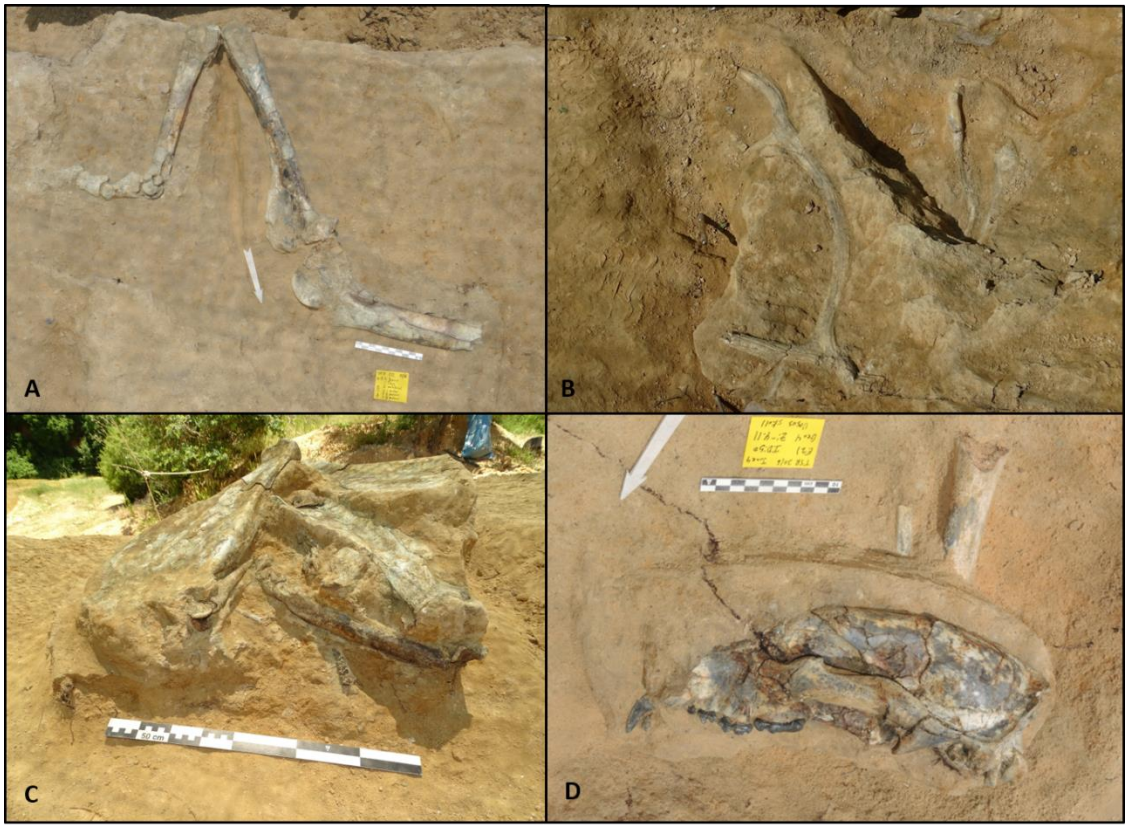

Figure 6. Tsiotra Vryssi: (A) Articulated leg (B) the herein studied cervid antler (TSR-D18-100) in situ (C) Cluster of various skeletal elements (D) Cranium (Ursus).

A late Villafranchian (Early Pleistocene) age is suggested for the TSR fauna (Konidaris et al., 2015, 2016; Kostopoulos et al., 2018; Koufos et al., 2018). This is supported by the presence of *Pachycrocuta brevirostris*, a large-sized hyaenid, which invaded Europe around 2.0 Ma (Martínez-Navarro, 2010). This invasion is known as "*Pachycrocuta brevirostris* event" and roughly coincides with the widespread distribution of the canid

Canis etruscus. Moreover, the presence of two equids, and the co-occurrence of the bovids *Leptobos* and *Bison*, indicate that the TSR fauna is of intermediate age between Gerakarou-1 [middle/late Villafranchian boundary (Koufos, 2014)], and Apollonia-1 [latest Villafranchian (Koufos, 2018)], both located in the Mygdonia basin. Consequently, Tsiotra Vryssi is dated to 1.8-1.2 Ma (Konidaris et al., 2015).

Table 1. Preliminary faunal list for TSR (adapted from Konidaris et al., 2015, 2016).

Class	Order	Family	Genus	Species
Reptilia	Chelonii	indet.		
Aves	Passeriformes	Corvidae	*Corvus*	*pliocaenus*
Mammalia	Carnivora	Canidae	*Canis*	*etruscus*
		Hyaenidae	*Pachycrocuta*	*brevirostris*
		Ursidae	*Ursus*	*etruscus*
	Perissodactyla	Equidae	*Equus*	sp. (medium-sized)
			Equus	sp. (large-sized)
		Rhinocerotidae	*Stephanorhinus*	sp.
	Artiodactyla	Giraffidae	*Palaeotragus*	sp.
		Cervidae	***Metacervocerus***	***rhenanus***
			Praemegaceros	
		Bovidae	*Bison*	sp.
			Leptobos	sp.
	Proboscidea	Elephantidae	*Mammuthus*	*meridionalis*

The preliminary study of the deer specimen from TSR indicated the presence of a small-sized along with a large-sized taxon. The former was originally represented by two upper tooth rows with P2-M3 and it was preliminary assigned to *Metacervocerus rhenanus* by Konidaris et al. (2015). The large-sized cervid remains were scarce; only a proximal phalanx was discovered at the time of the publication. Later on, the discovery of dental material permitted the attribution to the genus *Praemegaceros* (Konidaris et al., 2016). All above material and further specimens discovered during the subsequent years are studied herein in detail.

2. Research method

The description and system of measurements of the antlers follows the methodology of Heintz (1970) (Fig. 7). Dental terminology is according to Heintz (1970) and Gentry et al. (1999) (Fig. 8). The measurements of the mandible are based on the methodology of Croitor (2018) (Fig. 9). Upper case letters indicate upper cheek teeth and lowercase letters indicate lower ones.

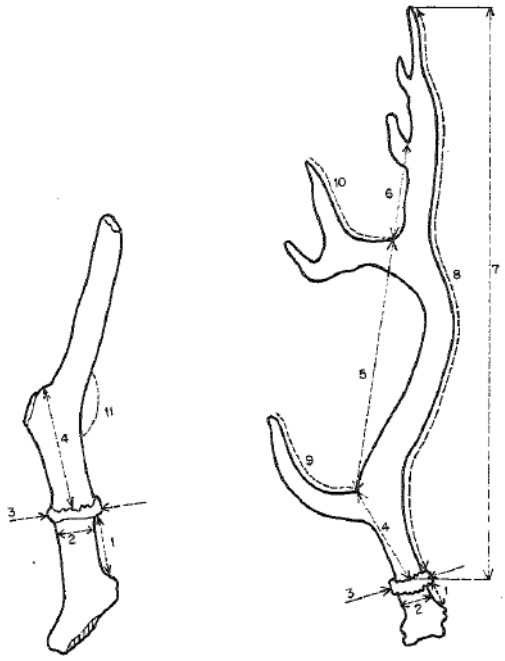

Figure 7. Left: Lateral-internal view of right antler of Arvernoceros ardei *(Etouaires), Right: Lateral-internal view of right antler of* Croizetoceros ramosus *(Etouaires). Measurements of the antlers from Heintz (1970). 1) Length of pedicle (2) Antero-posterior diameter of pedicle (3) Antero-posterior diameter of burr (4) Length of first segment (5) Length of second segment (6) Length of third segment (7) Total length in straight line (8) Total length following the curvatures (9) Length of 1st tine (10) Length of 2nd tine (11) Angle of the posterior edge of the beam.*

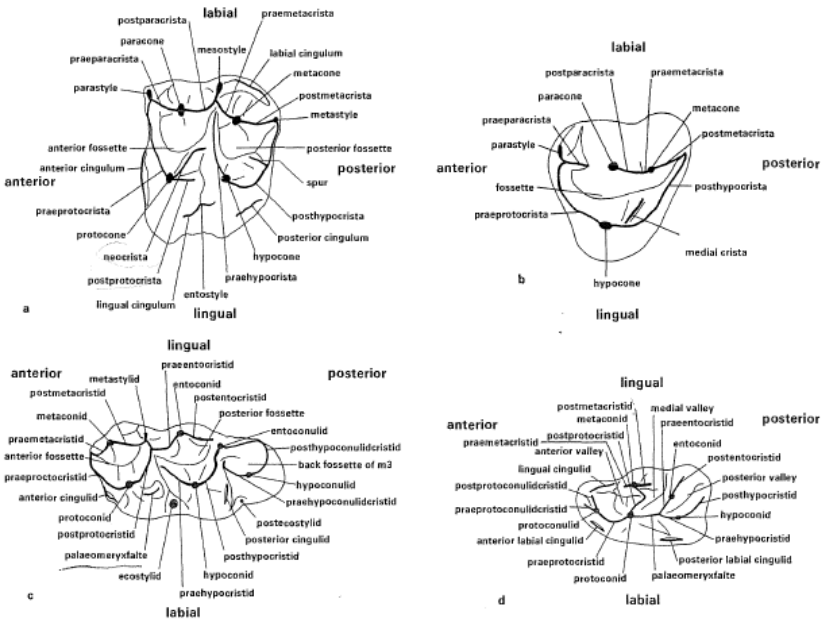

Figure 8. Terminology of tooth crown elements in ruminants (a) Upper second molar (b) Upper third premolar (c) Lower third molar (d) Lower fourth premolar. From Gentry et al. (1999).

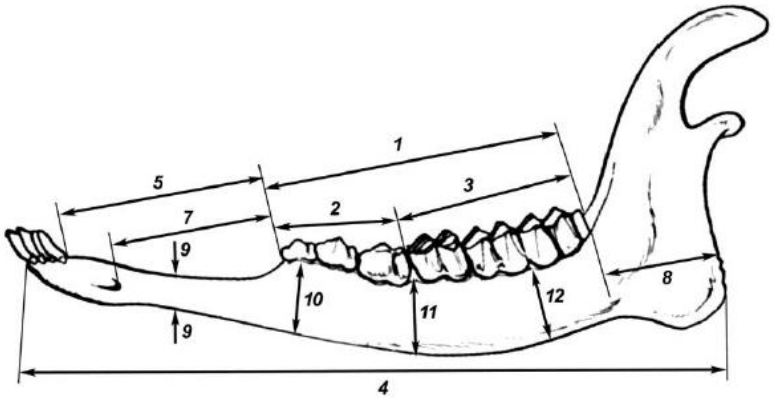

Figure 9. Measurements of the mandible. From Croitor (2018). (1) Length of the tooth row; (2) length of the premolar series; (3) length of molar series; (4) length of the mandibular corpus; (5) length of the diastema; (6, not shown) distance between p2 and the mandibular symphysis; (7) distance between p2 and the foramen mentale; (8) distance between m3 and the posterior edge of the mandible; (9) minimum height of the diastema; (10) height of mandible below p2; (11) height of the mandible below m1; (12) height of the mandible below m2-m3. Furthermore, the following measurements were included: (13, not shown) mandibular thickness below p2; (14, not shown) mandibular thickness below m1; (15, not shown) mandibular thickness below m2-m3.

For the postcranial skeleton we follow the measurements proposed by von den Driesch (1976), except for the metapodials, which are measured according to the system of Scott (2004) [see also Maniakas & Kostopoulos (2017); Fig. 10].

All measurements are shown in Tables 1-23 (Appendix I) and are given in mm. Measurements were taken by a digital caliper at 0.01 mm precision. Angles were measured by a digital goniometer at 0.1° precision. All data were analysed with the software PAST (Hammer et al., 2001). The illustrations and the images were processed with the graphic software Inkscape.

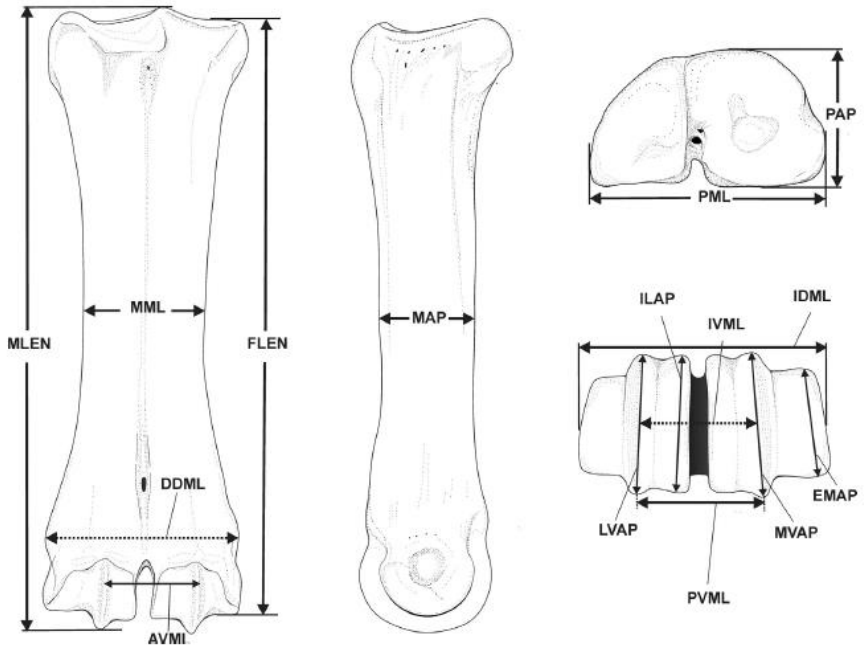

Figure 10. Illustration of metapodial dimensions following Scott (2004). MLEN: maximum length; FLEN: functional length; PAP: proximal epiphysis anteroposterior diameter; PML: proximal epiphysis mediolateral (transverse) diameter; MAP: midshaft (determined using MLEN) anteroposterior diameter; MML: midshaft mediolateral diameter; MVAP: medial trochear verticilli anteroposterior diameter; LVAP: lateral trochlear verticilli anteroposterior diameter; EMAP: external margin of medial trochlea; anteroposterior diameter; ILAP: internal margin of lateral trochlea anteroposterior diameter; AVML: anterior aspect of trochlear verticilli mediolateral diameter; IVML: distal diameter of trochlear verticilli mediolateral diameter; PVML: posterior aspect of trochlear verticilli mediolateral diameter; IDML: inferior aspect of distal epiphysis greatest mediolateral diameter; DDML: diaphysis distal end (metaphysis) mediolateral diameter. From Maniakas et al. (2017).

3. Systematic Palaeontology

Family Cervidae GOLDFUSS, 1820

Subfamily Cervinae GOLDFUSS, 1820

Genus *Cervus* LINNAEUS, 1758

3.1 *Cervus* sp. nov.

I. Material

***Antlers*.** Pair of antlers (TSR D18-100), right second tine (TSR D17-41), antler beam (TSR-167) and other fragmented parts of tines (TSR D18-100, TSR D17-35). The mentioned material belongs to adult individuals, except from the antler beam TSR-167.

Dentition. Fragmented left maxilla with P2-M3 (TSR-156), fragmented right maxilla with dP2-M1 (TSR G16-38), fragmented left maxilla with P2-M3 (TSR-135), two isolated left M1 (TSR G16-8 and TSR D17-44), and one isolated fragmented right M3 (TSR E18-24), complete right hemi-mandible with p2-m3 (TSR D18-99), fragmented left mandible with p3-m2 (TSR E13-5), fragmented right mandible with p2-m2 (TSR F20-49). The aforementioned material belongs to adult individuals (permanent dentition), except from TSR G16-38 which belongs to a young individual (bearing deciduous dentition).

Postcranial skeleton

- right calcaneum, cuboscaphoid and metatarsal (TSR H17-24c, 24a, 24b) of the same individual;
- left femur, tibia, patella, calcaneum, astragalus, cuboscaphoid, metatarsal, lateral phalanx I and medial phalanx II (TSR D18-48, 50, 53, 54, 52, 51, 55, 56), of the same individual;

- distal epiphysis of right tibia, tibial malleolus, astragalus, cuboscaphoid, metatarsal, lateral and medial phalanges I, II and III (TSR C18-13 and C18-10) of the same individual;
- distal epiphysis and part of diaphysis of right tibia, calcaneum and astragalus (TSR D18-84, 81, 83) of the same individual;
- distal epiphysis and part of diaphysis of left tibia, astragalus, cuboscaphoid, metatarsal, lateral phalanx I, lateral and medial phalanges II, lateral and medial phalanges III (TSR D18-103, 101, 102) of the same individual;
- right cuboscaphoid, sesamoid, metatarsal (TSR C18-9a, 9b, 9c) of the same individual;
- fragmented right scapula, distal epiphysis of humerus , ulna, radius capitotrapezoid, semilunaire, pyramidal, pisiforme, scaphoid, metacarpal, lateral and medial phalanges I, lateral phalanx II (TSR H17-22f, 22e, 22d, 22c, 22g, 22b, 22a) of the same individual (young);
- fragmented proximal part of left ulna (TSR D18-107) and fragmented distal epiphysis of humerus (TSR D18-107), of the same individual;
- fragmented left fragmented humerus (TSR-149);
- proximal epiphysis and part of diaphysis of right metacarpal (TSR C16-27), young individual;
- distal epiphysis of right tibias (TSR D18-117, TSR-110, TSR H17-12, C17-45);
- proximal epiphysis and part of diaphysis of left metatarsal (TSR-168);
- proximal epiphysis of left metatarsal (TSR-15);
- left calcanei (TSR C16-21, TSR D18-34);
- right astragalus, calcaneum and cuboscaphoid (TSR E17-8a, 8b, 8c) of the same individual;
- right astragalus and malleolus (TSR H17-14a) of the same individual;
- right astragalus (TSR F17-34);
- right cuboscaphoid (TSR C17-24);
- left cuboscaphoid (TSR C17-39a) and left proximal phalanx (TSR C17-39b) of the same individual;
- lateral and medial phalanges I (TSR D18-97) of the same individual;

- lateral and medial phalanges I and II (TSR 100) of the same individual;
- lateral and medial phalanges I, II and phalanx III (TSR-143) of the same individual;
- phalanges I (TSR-14, TSR D17-40, TSR D18-110, TSR D18-115, TSR C17-47, TSR-194, TSR-140, TSR-5);
- phalanges II (TSR C18-20);
- phalanges III (TSR G17-33, TSR C16-12, TSR D18-35, TSR-111, G17-34)

II. Taphonomic observations

The remains of the small-sized cervid include a total of 108 identified specimens (NISP). As shown in Figure 11 the most abundant are the phalanges, whereas the scapula, the humerus, the radius/ulna and the metacarpal remains are among the scarcer specimens. The Minimum Number of Individuals (MNI) corresponds to six adult and two young individuals (Tables 2 and 3, respectively).

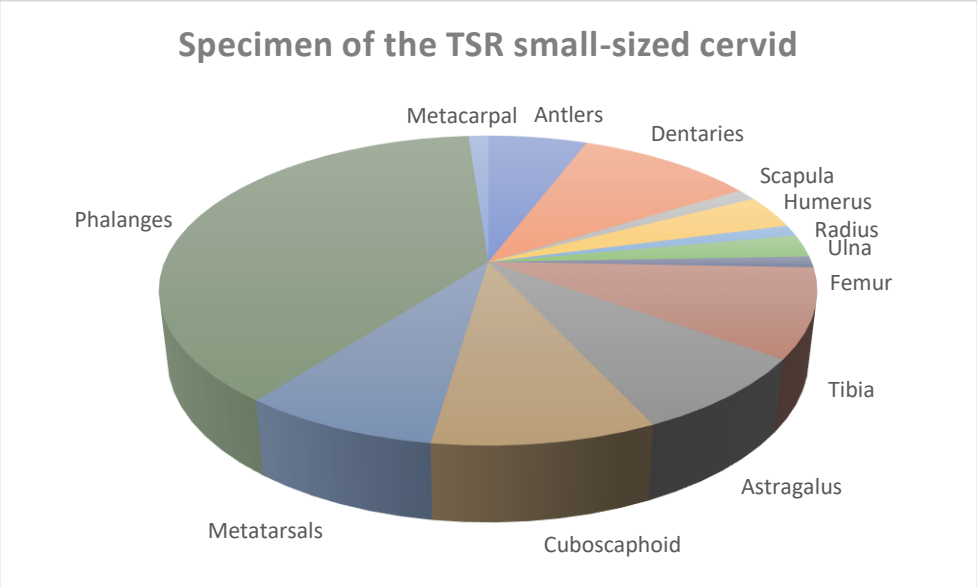

Figure 11. Relative abundance of the skeletal remains of Cervus *sp. nov. from TSR.*

Table 2. MNI per skeletal element of adult specimens of Cervus *sp. nov. from TSR.*

Bone type/Specimen	LEFT	RIGHT	MNI
Pair of antlers	X	X	1
Maxilla (P2-M3)	X	X	
Isolated M1	XX		4
Isolated M3		X	
Mandible (complete)		X	2
Mandible (p3-m2)	X	X	
Humerus	XX	X	2
Femur	X		1
Tibia	X	XXXXXX	6
Tibia	X		
Metatarsal	XXXX	XXX	4
Astragalus	XX	XXXXX	5
Cuboscaphoid	XXX	XXXXX	5

Table 3. MNI per skeletal element of juvenile-young specimens of Cervus *sp. nov. from TSR.*

Bone type/Specimen	LEFT	RIGHT	MNI
Antler beam			1
Maxilla (dP2-M1)		X	1
Metacarpal		X	2
Scapula/Humerus/Ulna/Radius/Metacarpal		X	

The following charts indicate the state of preservation of the tibias (Fig. 12) and metatarsals (Fig. 13) of the small-sized TSR cervid. These specific bones were selected due to their relative abundance within the whole collection. The metatarsals are represented in almost their entirety by complete specimens, whereas the tibias are represented by fragmented specimens, which preserve only the distal epiphysis. All astragali, calcanei and phalanges are represented by complete specimens.

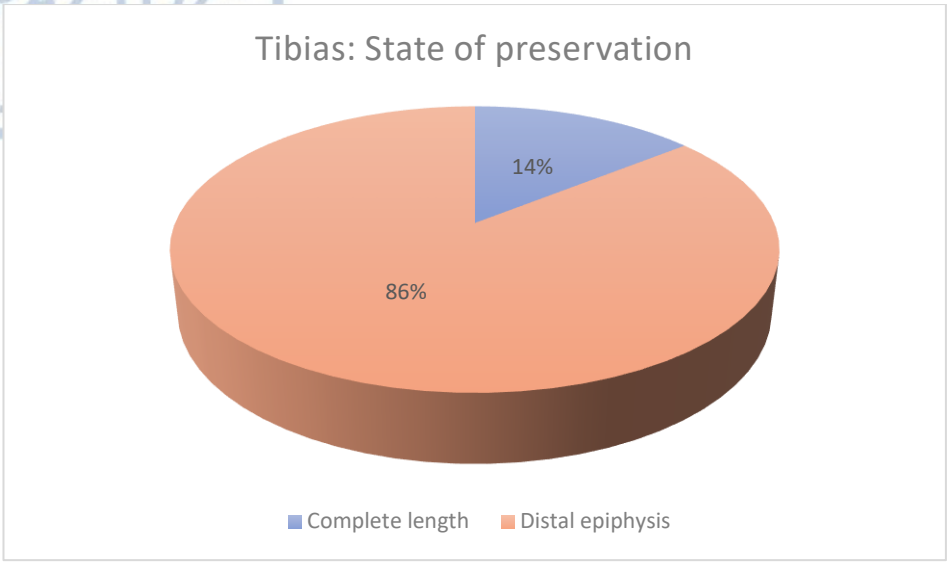

Figure 12. Pie chart indicating the state of preservation of the tibia remains of Cervus *sp. nov. from TSR.*

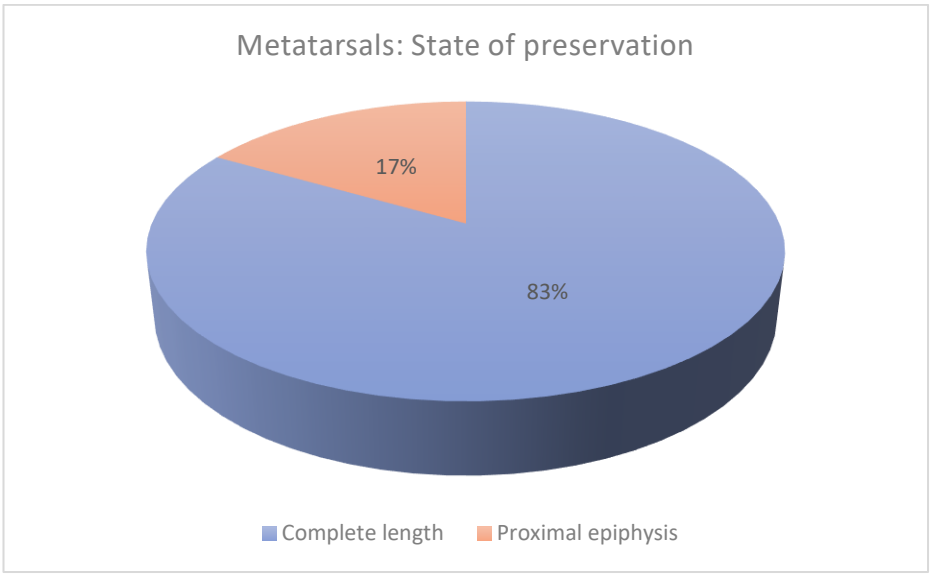

Figure 13. Pie chart indicating the state of preservation of the metatarsal remains of Cervus *sp. nov. from TSR.*

A great part (58 out of 89) of the identified postcranials take part of series of bones in anatomical connection, representing 8 legs (6 posterior and 2 anterior) preserved in a greater or lesser degree.

The percentages that appear on the charts (Figs. 6, 7) could be explained, considering the chewing pattern of the predators. In order to determine the patterns of carcass utilization, we take into account the relative food value of each skeletal part of the

bone. Certain skeletal parts of the carcass such as the cranium, the metapodials and the phalanges have a high bone/meat ratio (Davis, 2010). On the contrary, the upper leg bones (humerus and femur), the lower leg bones (radius, ulna and tibia), along with ribs and vertebrae are skeletal parts that bear significant muscle masses, increasing the preferability of carnivores in consuming them.

In addition, certain skeletal parts consist of higher percentages of grease. A study based on the Food Utility Index (FUI) for the quantity of meat, marrow and grease of the bones of the caribou, showed that certain skeletal parts rank higher than other (Metcalfe & Jones, 1988). Some of the highest ranked skeletal parts include the proximal and distal ends of the femur, the sternum, the proximal end of the tibia and the ribs, whereas the lower ranked skeletal parts are the cranium, the metatarsals, the phalanges and the dentaries.

All the above, along with the confirmed presence of large carnivores, e.g., *Pachycrocuta brevirostris* and *Canis etruscus* in TSR, could explain the selective state of preservation of the skeletal remains of the TSR small-sized cervid.

III. Description

***Antlers*.** The antlers are medium-sized and four-pointed (Plate I, Figures 3-6). The measured height from the burr to the tip of the right antler equals to 600 mm and the total height of the left one equals to 520 mm. The right antler is terminated by a partly fragmented distal fork, whereas the left one is destroyed at about 100 mm above the second ramification. The total estimated height of the antlers would be approximately 700 mm.

The cross-section of both the burr and the pedicle is (sub)circular. The pedicles are relatively high, round (DT/DAP = 1) and slightly flattened anteroposteriorly. The first tine branches off relatively high above the burr at 55 mm (right antler) and 60 mm (left antler), as measured on the internal side. It is relatively thin, long (~220 mm of total length) and strongly curved. The first tine is oriented on the parasagittal plane with

slight deviation medially in its distal part. It forms a 105° angle with the beam. The beam is strongly curved and laterally flattened between the first and second tine, and bears a distinct longitudinal groove all along this sector on the lateral side. The surface of the beam and the tines is sculptured with ridges and furrows.

The second tine is well-developed, and it is situated rather high above the first ramification, at 360 (left antler) and 320 mm (right antler). The third tine is situated at 138 mm above the second one and forms an angle 74° with the beam. In the right antler, the second tine is crashed near the base. In the left antler, this tine is better preserved showing a clear deviation from the parasagittal plane towards the medial side. The distance between the first and second ramification is significantly longer than the distance between the second and the third ramification (~½).

The distal part of the right antler is terminated by a distal bifurcation, which is oriented in the parasagittal plane. The fork is formed by two unequally developed tines, with the posterior being longer and slightly thicker than the anterior one. The two tines form an angle of 80°. In Figure 14 we illustrate the external sides of the antler specimens (TSR D18-100).

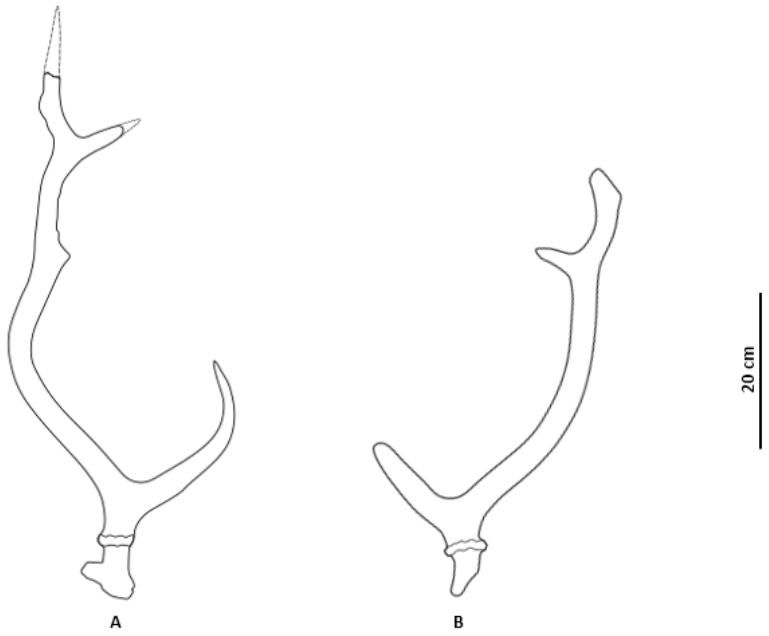

Figure 14. Illustration of the external sides of (A): the right and (B): the left antler of the TSR small-sized cervid.

The isolated antler beam (TSR-167) belongs to a young individual (Plate I, Fig. 2). Its length equals to 240 mm. It is straight-shaped, from the base to the tip. The tip of the beam is sharpened. There are no traces of developing tines. The beam surface is sculptured with furrows from the base and up to 160 mm above it. Measurements of the antlers are given in Tables 1 & 2.

Upper dentition. The cheek teeth are low crowned, and the enamel is rippled (Plate II, Fig. 7). There are traces of cement in both the lingual and the labial sides. The total length of the upper tooth row equals to 85 mm and the premolar/molar length ratio is 74-80% (n=2). Measurements are given in Table 3.

On the premolars, the hypocone and the protocone are well distinguished lingually, due to the advanced degree of molarization. The paracone of P2 and P3 is well developed, more prominent than on P4. The parastyle is thin on P2 and it increases toward P4. The metastyle is well developed and in P4 it is equally developed with the parastyle. In P4 the hypocone and the protocone do not separate (low/absent molarization). All premolar's fossetes are supplemented in with a distal enamel fold (hypoconal spur). The P3 and P4 of both available specimens bear a basal central cingulum on the lingual wall.

Lingually, all molars have strongly developed cingulum on the mesial wall and between the lobes. The cingulum appears more prominent in M2 and M3, where it forms well-developed, large double basal pillars. The protocone and the hypocone of the molars are angular, especially on M1 and M2, where the protocone appears more mesially oriented than the hypocone. The parastylid is more prominent than the metastylid. The mesostylid of the molars is equally developed with the parastylid. In M2 and M3 the mesostylid is parallel to the vertical plane and the parastylid is posteriorly inclined near the base, maintaining approximately the same breadth. All molar's fossetes are supplemented in with a distal enamel fold (hypoconal spur). On the less worn dentition (TSR-156), the postprotocrista of M2 and M3 is bifurcated.

Lower dentition. The total length of the lower tooth row equals to 88 mm (Plate II, Figures 8-10) The premolar/molar length ratio is 62% (n=1). The cingulum is reduced/absent, especially in m3. The tooth row is supplemented by a thin coat of cement. Measurements are given in Table 4.

In p2, the paraconid and the parastylid are not separated. The metaconid is narrow-elliptical and distally inclined. The entoconid and the entostylid are equally developed. The hypoconid is weakly developed in the labial side. The p3 and p4 hold well-separated protoconid from hypoconid. On p3 the parastylid and the paraconid are distinct only in the upper part of the crown. The entoconid is quickly fused with the entostylid, closing the distal valley. The metaconid of p3 directs distally and has an oval/(sub)elliptical shape. p4 is molarized, with well distinguished hypoconid from protoconid. The metaconid extends mesially (TSR F20-49) or mesio-distally (TSR E13-5). The variably developed paraconid extends distally; in TSR F20-49 the trigonid is still open lingually in the upper half of the crown, whereas in TSR E13-5 and TSR D18-99 it is closed. The entoconid is well distinct, the entostylid is very thin–they merge closing the distal valley. In TSR E13-5 and TSR D18-99, the metaconid gets in touch with the entoconid, providing a continuous lingual wall, and indicates an advanced dental pattern.

Molars bear basal pillars, single on m3 and double or flattened single on m1. The protoconid and the hypoconid of the molars are angular, and distally oriented. The lingual wall is slightly undulated. The third lobe of m3 is well-developed, sub-quadrate/rhomboid shaped.

The complete mandible is slightly fragmented in *processus angularis*. All measurements are given in Table 5.

Postcranial skeleton. The humerus remains are relatively poor (Plate III, Fig. 1). The proximal part (head) is spherical-shaped. On the distal part, the external condyle is smaller and narrower than the internal. There is a slight depression/groove on the median gorge, and overall the gorge is progressively raising, compared to the external

condyle. The external crest is well-developed and prominent. The olecranon fossa is deep and with a convex/cyclical outline. Measurements are given in Table 6.

The radius remains are represented by one complete specimen (TSR H17-22d), which belongs to a young individual (Plate III, Fig. 1). On the distal part of the diaphysis, there is an ulna fragment, which extends to the distal epiphysis of the radius. The posterior surface of the diaphysis is sculptured with a groove. Measurements are given in Table 7.

The remains of metacarpal bones are poor (Plate III, Fig. 1). The specimen (TSR C16-27) is fragmented; it bears the proximal epiphysis and part of the diaphysis. The posterior surface of the metacarpal is concave, and the anterior surface is smooth and lacks traces of a groove. The proximal epiphysis consists of two facets, a subquadrate medial for trapezoid-magnum and a subtriangular lateral one for hamate/unciform. Measurements are given in Table 8.

The femur remains include one complete specimen slightly fragmented in the proximal epiphysis (TSR D18-48) (Plate IV, Fig. 1). The proximal condyle (head) is cylindrical-shaped. Two crests that form a groove, are prominent from the proximal part of the diaphysis and above the distal part of it. On the anterior distal part, the lateral epicondyle is narrower and more cylindrical than the medial one. The intercondyloid fossa is relatively deep and triangular-shaped. Measurements are given in Table 9.

In almost all the tibia remains, only the distal part is preserved. The complete specimen TSR D18-50 is relatively slender (Plate IV, Fig. 1). The typical cervid features are observed (Heintz, 1970): the tibial crest is long and extended in terms of height. In the posterior surface of the bone, there is a narrow crest extending from the proximal to the middle part of the diaphysis. From the proximal to the medial part of the bone, the crest is progressively becoming less prominent. Starting from the middle of the diaphysis to the distal part, extend/s a prominent groove/two crests. On the distal part of the diaphysis, the groove is deep and well-developed. On the proximal epiphysis, the

angle between the articular facet and the tibial crest is almost 90°. The articular facets are deep, narrow and parallel to each other. Measurements are given in Table 10.

The astragali are relatively robust (in respect to the size of the animal) (Plate IV, Fig. 2) and they hold the typical cervid features (Heintz, 1970): the internal condyle is smaller and narrower than the external one. The horizontal part of the external condyle ascends abruptly with the median gorge; the internal condyle ascends more progressively to the median gorge. Also, the median gorge is shifted in the medial part of the bone. The outline of the condyles is convex. The above features create a relatively asymmetric profile of the astragalus. The outline of the lateral side is narrower, while the outline of the medial side is parallelogramed-shaped. The distal trochlea is somewhat symmetrical with the lateral part being slightly more extended and flattened than the medial part. Measurements are given in Table 11.

The calcanei are elongated and narrow (Plate IV, Fig. 2). The diaphysis is straight shaped from the lateral view. The first facet for the astragalus is positioned in the inferior side and it is slightly convex. The second facet for the astragalus faces medially and it is elongated, flattened and narrow. The lateral malleolar articular facet is relatively inflated, and it projects laterally. The articular facet for the cuboscaphoid is elongated, flattened and curved. At the proximal and posterior part of the bone (calcaneal tuberosity), there is a well-developed, relatively deep groove. Measurements are given in Table 12.

In the dorsal side of the cuboschaphoids (Plate IV, Fig. 2), the articular surface for the astragali has two depressed areas, while at the lateral side extends the convex calcaneal articular surface. Ventrally, the 1st articular faced for the metatarsal is located laterally and has a sub-parallelogram shape. The second is smaller, located in the lateral side of the posterior part, and has an elongated flattened shape. The articular facet for the intermediate/lateral cuneiform is deep and oval shaped. The articular facet for the medial/small cuneiform is somewhat oval but with a progressive narrowing at its posterior side. Measurements are given in Table 13.

The metatarsals are slender (Plate IV, Fig. 3). The Robustness Index (DT diaph. /GL %) equals to 7.8 (n=5). The proximal epiphysis is subquadrate. The posterior surface of the diaphysis is concave. Dorsally and above the distal part, there are crests on both sides of the metatarsal sulcus. There is a relatively deep groove on the anterior surface of the diaphysis. The shaft is transversally compressed, especially on the proximal part of the diaphysis. In proximal epiphysis, the medial facet for the cuneiform magnum extends and overlays the lateral facet for cuboscaphoid. The anterior surface of the medial part of the fused metatarsal is more prominent than the anterior surface of the lateral part. The distal part of the metatarsal is inflated above the low articular surfaces. Measurements are given in Table 14.

The proximal phalanges are relatively robust, with a Robustness Index equal to 24.5 (n=16). The proximal articular surface is relatively broad with a weak incision for the metapodial verticili. There is a weak groove in the internal side. The outline of the dorsal surface is straight. The outline of the distal articulation is somewhat rounded. The facet of the distal articulation is partly visible from the dorsal aspect. The outline of the volar side is relatively straight as observed from the interdigital side. The external side is concave from the dorsal aspect. Measurements are given in Table 15.

The middle phalanges are also relatively robust. The Robustness Index equals to 34 (n=8). The proximal articular facet is weakly concave from the lateral side. In the proximal part, the dorsal (extensor) process is relatively short. The outline of the distal articular surface is rounded. Dorsally and palmarly it extends slightly. On the palmar side, the surface is relatively smooth and lack of a sagittal groove. Measurements are given in Table 16.

The distal phalanges are triangular shaped from the lateral side. The dorsal ridge is almost straight, with a very weak angle, forming a slightly convex outline. The process for the insertion of Extensor tendon is sharp and not particularly developed. The articular surface is rounded, not very deep. The dorsal ridge is long with an inclination to the interdigital side. Measurements are given in Table 17.

Body mass. The body mass of the TSR small-sized cervid is estimated at about 75 kg (mean), by selected predicting equations (Table 4), as given by Janis (1990) for dentaries.

Table 4. Equations used for estimation of body mass in the small-sized TSR cervid, as proposed by Janis (1990).

Equation	Body weight (kg)
Log (BW) = 3.218 × log (LM2) + 1.073	78
Log (BW) = 3.334 × log (Lm1) + 1.270	72
Log (BW) = 3.106 × log (Lm2) + 1.119	77

IV. Comparison with small & medium-sized Plio-Pleistocene cervids of Europe

The systematics and classification of the small-sized European Plio-Pleistocene cervids has been a debatable issue, due to the polychotomous scientific points of view. Since consensus has not been yet achieved into classifying these cervids, some of the genera appear problematic.

This is the case of *Praeelaphus*, which was supposed as synonymous with *Metacervocerus* by Grubb (2000). Croitor (2018), states that the two genera are different, because *Praeelaphus* is based on *Cervus perrieri* CROIZET & JOBERT, 1828 and *Metacervocerus* is based on *Cervus pardinensis* CROIZET & JOBERT, 1828. *Cervus perrieri* was at first placed by Heintz (1970) in the group *Cervus sensu lato*. Croitor (2012) applied the genus name *Praeelaphus*, with *C. perrieri* as the type species, including other related forms.

Another quite problematic taxon is *Cervus nestii* AZZAROLI, 1947, which was originally described by Azzaroli (1947) as *Dama nestii nestii* AZZAROLI, 1947. The same author, at 1992, proposed the genus *Pseudodama* to include the *Dama*-like cervids. Pfeiffer (1992) considered it as a subgenus of *Dama*, but other authors recognized *Pseudodama,* with *Dama nestii nestii* as type species, as a valid and polyphyletic taxon.

According to Croitor (2018), *Pseudodama* includes primitive members of the genera *Cervus, Dama, Metacervocerus,* and *Praeelaphus*. Di Stefano & Petronio (2002) proposed that taxa included in "*Pseudodama*" belong in the modern genus *Axis*. However, this opinion was not adopted by the research community. In terms of simplicity, we follow in this work the taxonomic scheme proposed by Croitor (2018).

Antlers. The small-sized *Croizetoceros ramosu*s, the systematic position of which is still a debatable issue (Croitor, 2018), is clearly distinguished by all known Plio-Pleistocene cervids, due to its rather distinctive antler morphology: the first tine branches off notably high from the burr and the crown consists of a variable in number tines, placed anteriorly of the beam (Heintz, 1970). Such features are absent from the TSR taxon: the first tine is situated in a much shorter to the burr distance, and the distal bifurcation consists of two, anteroposteriosly oriented tines.

The genus *Praeelaphus* with the type species *Cervus perrieri* represents small and medium-sized deer with large, four-pointed antlers (respectively to the animal size) (Croitor, 2017). The main features displayed in the antlers of *Praeelaphus* are: (a) moderate pedicle length, (b) first tine situated above the burr, in distance longer than the diameter of antler base, (c) flattened portions of the antler beam (especially above the second tine), with a frontal, oblique or sagittal orientation (Croitor, 2017 2018). The antler beam is terminated by a distal bifurcation, with a frontal or sagittal orientation. The genus includes the species *P. perrieri; P. lyra* AZZAROLI, 1992; *P. warthae* CZYZEWSKA, 1968 and *P. australorientalis* CROITOR, 2017.

At first, compared to the antlers of *P. perierri,* the ones from TSR have a much more curved beam between the first and second ramification. In addition, the first and especially the second tine are inclined toward the medial side, unlike to *P. perierri,* where the tines deviate laterally. In the studied material, the distal fork is oriented in the sagittal plane, a feature that seems variable in *Praeelaphus* representatives (Croitor, 2017). Nevertheless, the orientation of the distal part of the beam clearly distinguishes the TSR small-sized cervid from *P. lyra*. The holotype of *P. warthae* is a damaged skull of a young individual, without antlers (Croitor, 2017). It is hypothesized

that the fully-grown antlers were four-pointed and terminated by a distal bifurcation (Croitor, 2018). Accurate comparison to this species with the TSR material is not possible.

The antlers of *P. australorientalis* differ notably from the rest of *Praeelaphus* group, due to the significantly high position of the first tine, the short distance between the first and second tines and the parasagittal position of the flattened, blade-like distal part of the beam (Croitor, 2017). More specifically, the distance between the first and the second ramifications equals to 1/3 of the distance between the second and the third ramification. The above features, along with the relatively straight antler beam of *P. australorientalis* distinguish it from the TSR cervid. It has to be noted, that according to Croitor (2017), the position of the distal part of the beam is a variable character in the case of *P.* cf. *lyra* from Olivola, Italy (Early Pleistocene), and could also be variable in the case of *P. perrieri*.

Croitor (2018) includes in the genus *Dama, D. eurygonos* AZZAROLI, 1947, *D. vallonnetensis* DE LUMLEY, KAHLKE, MOIGNE & MOULLE, 1988, *Dama clactoniana* FALCONER, 1868, and *D. carburangelensis* DE GREGORIO, 1925. Unlike the studied material, *Dama eurygonos* holds a robust pair of antlers terminated with a large distal fork. The first tine forms a very obtuse angle of 120° with the beam and branches off relatively close to the burr (Croitor, 2018). The distal fork in *D. eurygonos* is very large, and it is formed by two tines, a longer anterior and a posterior, unlike the studied material, where the tines are significantly shorter, with the posterior being longer than the anterior one. Also, in *D. eurygonos*, the distance between the first and middle tine equals to the distance between the middle tine and the distal fork, in contrast to the material from TSR, where the distance between the second and third ramification equals to approximately ½ of the distance between the first and second ramification. The crown tines of *D. eurygonos* are oriented in the parasagittal plane, similarly to the TSR cervid. Other species included in *Dama* (e.g., *D. dama, D. clactoniana, D. carburangelensis*), hold palmated antlers, in sharp contrast to the studied ones, whereas *Dama vallonnetensis* holds a three-pointed pair of antlers.

According to Croitor (2018), *Cervus nestii* is among the earliest representatives of the genus *Cervus* in the Villafranchian of Europe. It holds long, four-pointed antlers, which are terminated by a distal bifurcation formed by two equal in size tines, unlike the TSR taxon. In addition, the distal fork in *C. nestii* is oriented in the frontal plane, and not sagittally, as in the studied pair. In *C. nestii*, the first segment of the beam is longer than the second, but not in ratio equal to 2:1, as observed in the studied antlers. Finally, the second and the third tines in *C. nestii* deviate laterally, whereas in our material, these tines and especially the second one, curves to the medial side. *Cervus abesalomi* KAHLKE, 2001 from the Early Pleistocene of Dmanisi (Georgia) is not significantly different from *C. nestii,* and hence it is distinguished from the TSR sample by the same set of differential features.

Cervus canadensis ERXLEBEN, 1777 and *Cervus elaphus* LINNAEUS, 1758 are two large-sized Middle-Late Pleistocene to present cervids that differ from the TSR taxon due to their large body size. The antlers of *C. canadensis* are terminated by a comb-like crown with three tines, situated in the parasagittal plane. The antlers of *C. elaphus acoronatus* BENINDE, 1937 are terminated by a distal fork oriented in the transversal plane as in *C. nestii. Cervus elaphus angulatus* BENINDE, 1937 is characterized by a peculiar distal crown. There is an initial distal fork with an additional long caudal tine that sometimes forms up to six tines ("*acoronatus*-type"). The above features furthermore distinguish the mentioned species from the TSR cervid.

The genus *Metacervocerus* with type species *Cervus pardinensis,* includes small-sized primitive deer of the late Pliocene-Early Pleistocene of Europe (Croitor, 2018). Their antlers are simple and three-pointed, unlike the TSR taxon. Nevertheless, the antlers of *M. pardinensis*, as well as of *M. rhenanus* DUBOIS, 1904; display certain similarities to the TSR cervid: the relatively high position of the first tine above the burr, the parasagittal orientation of the distal bifurcation, the longer and stronger posterior tine, the lateral compression of the antler beam in the distal area, along with longitudinal grooves that sculpture the antler beam.

The proportions of the pedicle of selected small to medium-sized cervids are shown in the following graph (Fig. 15). Except from *D. eurygonos* (with relatively shorter pedicels) and *P. perrieri* (with larger ones), the rest of the compared cervids share similar in size pedicles.

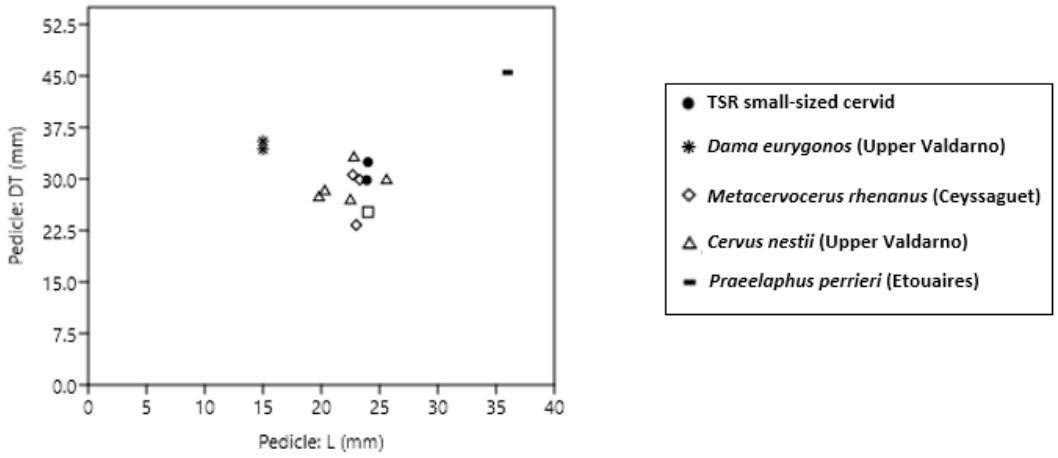

Figure 15. The relative proportions of the pedicles in Plio-Pleistocene small-sized cervid of Europe.

Dentition. In general, there are no significant differential dental features between the TSR cervid and other Plio-Pleistocene European deers. Nevertheless, in this section we compare some main dental patterns, taking into consideration that some of them are variable even in a species level. From a metric point of view, the measurements of the TSR cervid dentition fall within the range of other small-sized Plio-Pleistocene European deer.

Metrical Observations

Cervus elaphus and *C. canadensis* are excluded from the following comparison due to their sizable differences with our material, e.g., *Cervus canadensis* bears a lower tooth row with length equal to 151.8 mm (Croitor, 2018), much larger than that of the TSR cervid, where the p2-m3 length equals to 88.02 mm (~1/2).

The lower premolar series of the *Praeelaphus* species is relatively long. The premolar/molar ratio of *P. perrieri* ranges from 64.3 % to 70.8 %; the TSR ratio is slightly shorter, equal to 62%. *Praeelaphus lyra* and *P. australorientalis* are only known by antler remains (Croitor, 2017).

The lower tooth row of *Dama eurygonos* has a length of 91.0 mm (Croitor, 2006) and a lower premolar/molar ratio of 62.6%, both values comparable to that of TSR cervid (88.02 mm; 62%).

The lower premolar/molar ratio of *Cervus nestii's* mandible equals to 64.3% slightly larger than in TSR. The length of the upper molars of *Metacervocerus pardinensis* equals to 53 mm (Heintz, 1970); in the TSR taxon it equals to 49 mm in average (n=3). The lower tooth row (p2-m3) of *M. rhenanus* varies from 84.8 to 100.1 mm; the TSR specimen falls closely within this range (= 88.02 mm). According to Croitor (2006), the lower premolar/molar ratio equals to 61.4-65.8%, similarly to TSR cervid (62%).

Praeelaphus perrieri is distinguished by the other cervids due to its larger relative length of the upper and lower tooth row. The TSR taxon bears a larger tooth row compared to *Dama eurygonos* and falls relatively close to *Metacervocerus rhenanus* (Figures 16 & 17).

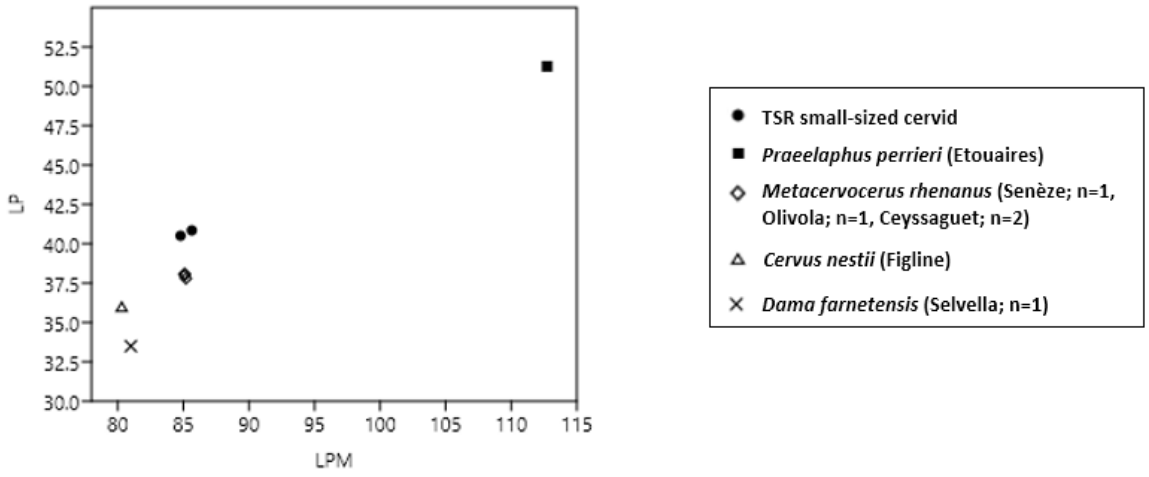

Figure 16. Relative measurements of the upper tooth row (LPM) and the upper premolar length (LP) of small-sized cervids. All measurements are given in mm.

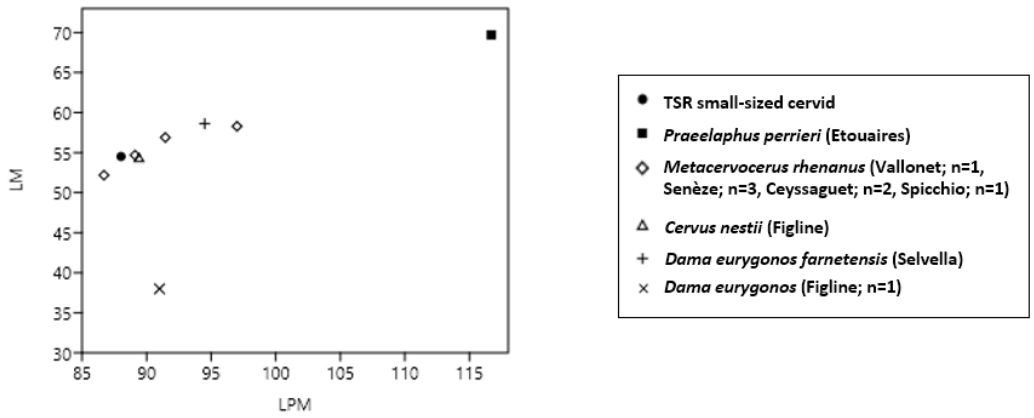

Figure 17. Relative measurements of the lower tooth row (LPM) and the lower molar length (LM) of small-sized cervids. All measurements are given in mm.

Morphological Observations

(a) Upper dentition

In *Praeelaphus warthae*, the hypocone and protocone of P3 are separated and the hypocone is supplemented with enamel folds; both features are present in the TSR specimens. P4 is supplemented with a bifurcated hypoconal enamel fold, whereas in the TSR cervid the hypoconal spur is not bifurcated. *Praeelpahus warthae*'s upper molars are supplemented with small entostyles and hypoconal spurs, similarly to the TSR taxon; however, they have also small enamel folds on the posterior and the anterior wing of the protocone, unlike the TSR taxon. As a whole, *P. warthae* seems to have a more complicated upper dental morphology (Heintz, 1970).

Cervus nestii's molars are advanced (Croitor, 2006). The upper molars are characterized by weak cingulum and small entostyles, unlike the TSR taxon, where the strongly developed cingulum forms large basal pillars. The upper molars have no enamel folds, whereas in the TSR taxon the fossettes bear hypoconal spurs. The *Palaeomeryx* fold is absent in both taxa.

In the upper molars of *Dama eurygonos*, the cingulum is weak, interrupted in the lingual side of the molars and it appears stronger in M1; on the contrary, in the TSR cervid the cingulum is strongly developed in the mesial and lingual side of the molars – more prominent in M2 and M3. The M3 of *Dama vallonnetensis* lacks enamel folds, as well as well-developed cingulum; contrarily to TSR cervid.

Metacervocerus pardinensis bears a primitive dentition (Croitor, 2006). Its upper molars and P4 are characterized by a strong cingulum, which forms a "zone" around the teeth in the lingual side (Heintz, 1970). Such a feature is absent in the TSR taxon. The upper molars of *M. pardinensis* are also supplemented with protoconal fold (absent in TSR material) and hypoconal spurs (present in TSR material). All upper premolars bear separated protocone and hypocone, less developed in P2, as in the TSR cervid.

Metacervocerus rhenanus bears a P2 with well separated protocone and hypocone – the latter with an enamel fold, as in the TSR cervid. The hypocone and the protocone of P3 are separated by a vertical groove and the hypoconal spur is present similarly with the TSR specimens. In P4, the hypocone and the protocone are not separated; in TSR material there is a vertical groove in between them. The upper molars of *M. rhenanus* are characterized by the presence of entostyles; M2 and M3 of the TSR taxon bear entostyles as well. The upper molars of *M. rhenanus* from Seneze, France are not supplemented with additional hypoconal or protoconal folds; unlike TSR cervid where hypoconal spurs are observed. A weak cingulum is variably present in Senèze, though in TSR taxon it is strongly developed. Nevertheless, the upper molars of *M. rhenanus* from Ceyssaguet (France) are supplemented with protoconal folds and spurs, along with a folded inferior enamel of hypocone (Croitor & Bonifay, 2001).

(b) Lower dentition

The lower dentition of the *Praeelaphus* species is primitive (Croitor, 2018): p4 shows a low degree of molarization unlike the molarized p4 of the TSR cervid. All the lower molars of *P. perrieri* have traces of cingulum and lack the *Paleomeryx* fold, as in the TSR

cervid (Heintz, 1970). Interlobar pillars are present on all the m1 and the m2, as in the TSR taxon. On m3, the basal pillar between the 1st and the 2nd lobes are always present, whereas between the 2nd and the 3rd lobes the pillars might be absent. On certain *P. perrieri* molars, the cingulum and the basal pillars are much better developed, in contrast to others. The internal wall of p4 is never completely closed, in contrast to the TSR cervid (Heintz, 1970).

In *P. warthae* the parastylid and paraconid are separated; in TSR cervid they are distinct only in the upper part of the tooth. The metaconid is extended mesio-distally and does not connect with the paraconid and the entoconid, unlike the TSR taxon where it gets in touch with the entoconid. Both *P. warthae* and the TSR taxon bear lower molars with ectostylids and lack the *Palaeomeryx* fold.

The species included within *Dama* are generally characterized by a molarized p4, as the TSR specimens. The metaconid extends mesio-distally and its anterior wing merges with the parastylid, unlike to the TSR taxon. The anterior valley is closed, like in the TSR specimen. As in the TSR specimens, the paraconid is not developed and the entoconid with the entostylid get in touch, forming a closed posterior valley. In *D. eurygonos* lower molars bear small ectostylides; in TSR cervid large basal pillars are present. The p4 of *D. vallonnetensis* is also advanced: the anterior wing of the metaconid gets in touch with the paraconid. The metaconid does not extend porsteriosly; in the TSR taxon it extends mesially or mesio-distally.

In *Cervus nestii*, p4 bears not well-separated parastylid and paraconid, unlike our material. In *C. nestii* the lower molars are characterized by ectostylides, as in the TSR taxon.

The morphology of the p4 of *Metacervocerus pardinensis* is primitive (Croitor, 2018); contrarily to the TSR material. Lower molars of *M. pardinensis* are sometimes supplemented with a continuous cingulum, which is absent in TSR.

In *M. rhenanus*, the p4 is primitive and simple (Croitor, 2006); unlike the TSR specimens. Lower molars of *M. rhenanus* are supplemented with ectostylids and the *Palaeomeryx* fold is absent, similarly with the TSR taxon.

Postcranials. Based exclusively on metric data, we compared the relative proportions of the TSR astragalus and metatarsal with the ones of the aforementioned cervids (Figs. 18 and 19, respectively). The selection of this specific body parts was based on: (1) their relatively high abundance within the studied assemblage, and (2) their significance in the morphological analyses of body size of Artiodactyla (Scott, 1983). The relative dimensions of other body parts, e.g., the calcaneum and the phalanges, are highly associated with the habitat category of each taxon (Köhler, 1993; Curran, 2012); subsequently they provide less objective results in the study the body size.

As shown below, *Praeelaphus perrieri* bears quite larger astragali and metatarsals. The astragali of *Metacervocerus pardinensis* are also somewhat larger than those of the TSR taxon. The proportions of metatarsals of the TSR cervid fall quite closely to that of *Metacervocerus rhenanus* and *Dama eurygonos*, whereas they seem somewhat larger than *Cervus nestii* and smaller than *M. pardinensis*.

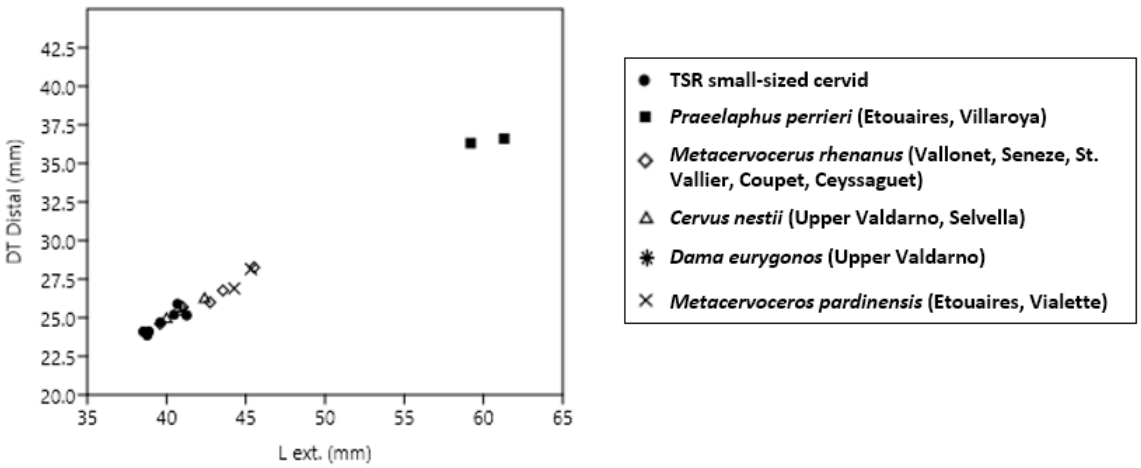

Figure 18. Relative proportions of the astragali of small to medium-sized European Plio-Pleistocene cervids.

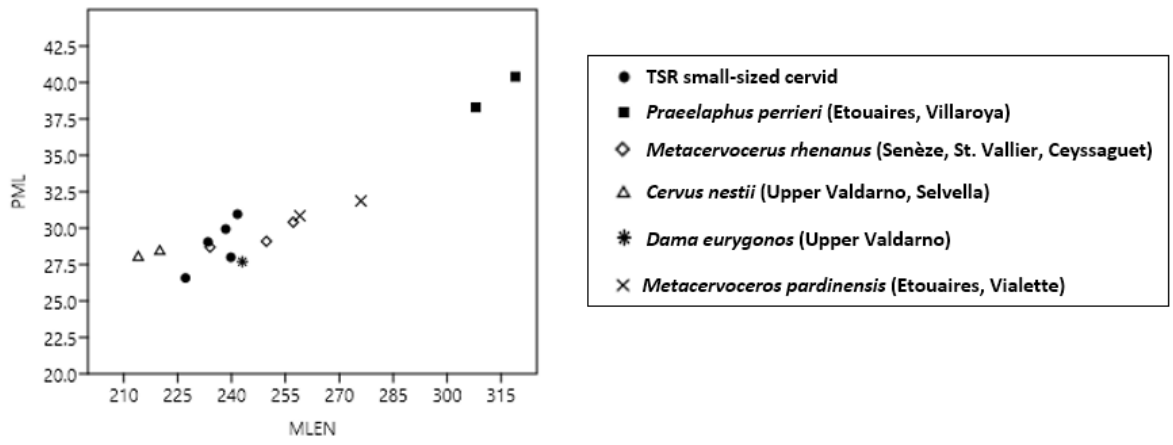

Figure 19. Relative proportions of the metatarsals of small to medium-sized European Plio-Pleistocene cervids. All measurements are given in mm.

Genus *Praemegaceros* PORTIS, 1920

3.2 *Praemegaceros* sp.

I. Material

***Dentition*.** Fragmented right maxilla with dP3-M2 (TSR E19-17).

***Postcranial skeleton*.** Fragmented distal epiphysis of right tibia (TSR H23-2); left astragalus (TSR D13-12); phalanges I (TSR H18-7, TSR D23-4); phalanx II (TSR-125) and phalanges III (TSR D18-36, TSR-37).

II. Description

Upper dentition. The maxilla (Plate V, Fig. 2) belongs to a young individual (dP3-M2). There are no prominent traces of cement in the lingual or the labial side. M2 is in early stage of wear, whereas the facets of dP4-M1 are in a more advanced wear state. The hypocone of dP3 is fragmented and its protocone is poorly preserved. The protocone of dP4 is fragmented in the labial side. Measurements are given in Table 18.

In the lingual sides of M1 and M2, the cingulum is weak/vestigial and interrupted between the lobes. M1 bears double basal pillars and M2 bears a well-developed basal pillar along with a second weak/vestigial one. The protocone and hypocone are angular shaped on M1, whereas on M2 they are slightly rounded, due to its unworn state. On M1 and M2 the mesostyle is very prominent and equally developed with the paracone rib. The mesostyle is inclined to the mesial side. On M1 and M2 the parastyle is also well-developed and prominent, with an inclination to the distal side. There is an enamel fold on the anterior fossete of the protocone of dP4, as well as a vestigial hypoconal spur in the unworn M2. Apart from the mentioned, there are no additional enamel folds on the upper tooth row.

Postcranial skeleton. The distal part of the tibia is robust (Plate V, Fig. 2). There is a groove on the medial side of the diaphysis, progressively becoming more prominent at the distal end. On the posterior surface of the diaphysis there are two grooves, which fade on the distal part of the bone. The distal facets are deep; the medial is narrow and the lateral is oval shaped. The medial malleolus surface is straight and extended on the distal end. Measurements are given in Table 19.

The astragalus is robust (Plate V, Fig. 3). The internal condyle is narrow; the external is broader and somewhat spherical-shaped. The median gorge is shifted in the medial and anterior side of the bone. In the middle of the anterior part of the diaphysis, there is a well-developed groove. The lateral part of the distal trochlea is slightly more extended and flattened than the medial part. Measurements are given in Table 20.

The proximal phalanges (Plate V, Fig. 4) are rather robust; the Robustness Index (DT diaph. /GL %) equals to 36.9 (n=2). The proximal articular surface bears a moderately deep incision for the metapodial verticillus. There are no traces of a groove in the dorsal part. The internal side of the diaphysis is rough [insertion of strong interdigital ligament Köhler (1993)]. From the dorsal aspect, the external side is concave. The distal articulation facets are partly visible from the dorsal aspect. The outline of the dorsal surface is straight. The distal surface has a well-rounded outline and the concave volar curvature begins below the proximal epiphysis. Measurements are given in Table 21.

The medial phalanx (Plate IV, Fig. 4) is robust, with a Robustness Index equal to 47 (n=1). The proximal articular surface is weakly concave as seen from the proximal aspect. The 'plateau postarticulaire' (Köhler, 1993), is elongated and protruded. The dorsal extensor process is short. On the internal aspect, the outline of the distal articulation surface is well-rounded. The distal articulation quietly extends dorsally and palmarly. On the palmar side there is absence of a sagittal groove. The interdigital part of the distal articulation is elongated. Measurements are given in Table 22.

The dorsal ridge of the distal phalanx (Plate IV, Fig. 4) is straight with a slight depression on its upper part. There is a somewhat strong protuberance for the extensor insertion. The articular surface is well rounded, situated rather high above the wedge. The dorsal ridge is of medium height, with an inclination to the interdigital side. Measurements are given in Table 23.

Body mass. The large-sized TSR cervid has a body mass of approximately 465 kg, as estimated by the predicting equation for the upper second molar, given by Janis (1990).

III. Comparison with large-sized Plio-Pleistocene cervids of Europe

The Early Pleistocene large-sized known cervid genera, are the closed related *Eucladoceros* and *Praemegaceros*, along with the poorly known genus *Arvernoceros* (Croitor & Brugal, 2007).

In Europe the genus *Eucladoceros* is represented by two species, *E. ctenoides* NESTI, 1841 (= *E. senezensis* DEPERET & MAYET, 1910) and *E. dicranios* NESTI, 1841. European continental species of *Praemegaceros* include *Praemegaceros obscurus* AZZAROLI, 1953; *Praemegaceros pliotarandoides* DE ALESSANDRI, 1903 and *Praemegaceros verticornis* DAWKINS, 1872. *Praemegaceros obscurus* is a common cervid in late Villafranchian European deposits (Croitor, 2018). *Praemegaceros pliotarandoides* was discovered in several pre-Galerian and Galerian faunas of South/Southeast Europe, including Apollonia-1 (APL) in Mygdonia basin [(Croitor & Kostopoulos (2004); Croitor

(2018)]. *Arvernoceros* contains the giant deer *Arvernoceros giulii* KAHLKE, 1997 and *Arvernoceros verestchagini* DAVID, 1992. The latter is also referred in APL faunal assemblage as *Arvernoceros* cf. *verestchagini* (Croitor & Kostopoulos, 2004).

In terms of body size, the TSR large-sized cervid (estimated body mass of 465 kg), falls within the range of *Praemegaceros* and *Arvernoceros* representatives, exceeding the usual body mass observed in *Eucladoceros*. The approximate body masses of the mentioned Early Pleistocene large-sized cervids are quoted in Figure 20.

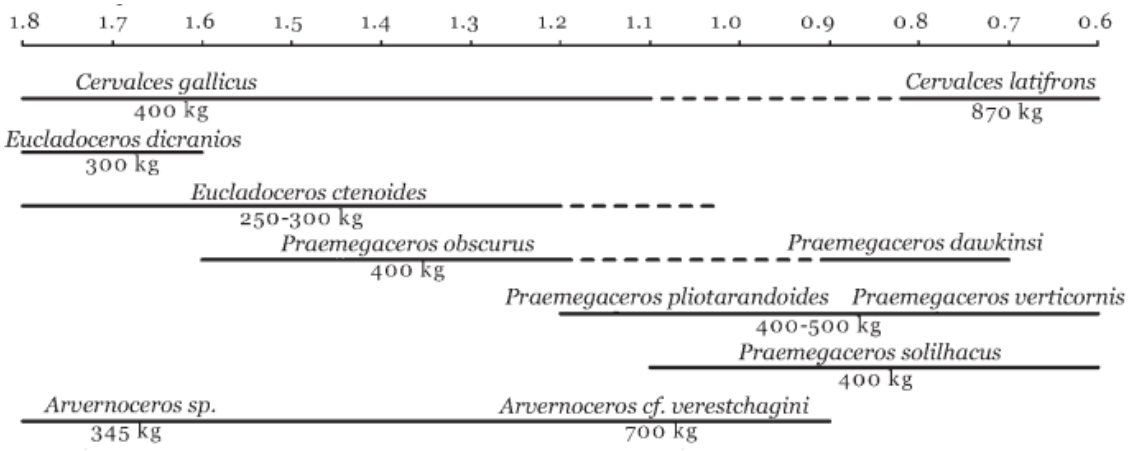

Figure 20. Distribution and estimated body mass of several Early Pleistocene large-sized cervids. Modified from Croitor & Brugal (2007).

Dentition

Metric observations. The maxilla of the TSR large-sized taxon belongs to a young individual and it is compared with selected representatives of *Praemegaceros, Eucladoceros* and *Arvernoceros*. In Figures 21 and 22, the relative proportions of the M1 and M2, respectively, of the mentioned large-sized deer are indicated.

As indicated, the M1 of the TSR large-sized cervid is relatively larger than the one of *E. ctenoides* as described by Heintz (1970) and *E. ctenoides* from Gerakarou-1 (Northern

Greece), as described by Kostopoulos (1996). It appears close in size with the M1 of *Praemegaceros verticornis* and *A.* cf. *verestchagini* (Fig. 20). The M2 of the TSR taxon is relatively larger compared to the M2 of the *Eucladoceros* representatives, and of similar size to *P. pliotarandoides* and *P. verticornis*.

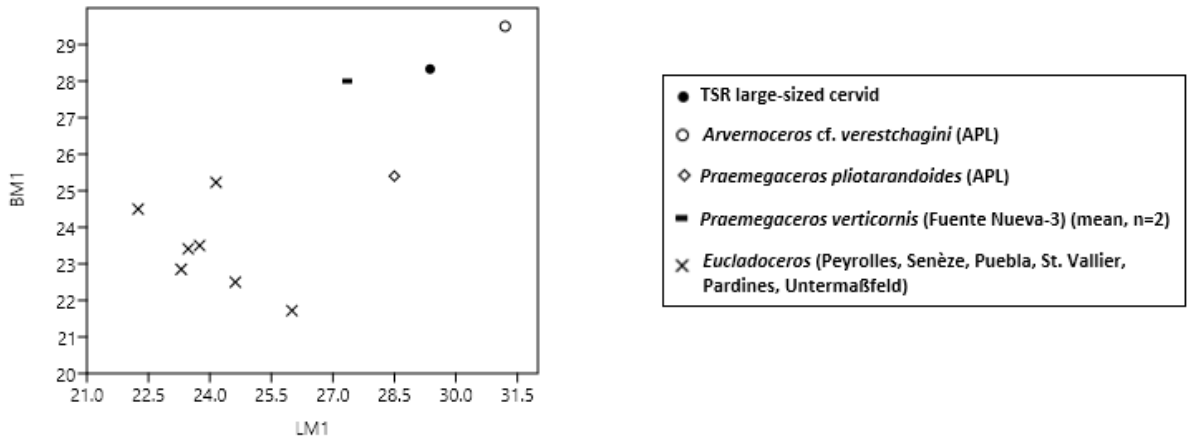

Figure 21. Relative proportions of M1 of large-sized Plio-Pleistocene cervids (L: Length, B: Breadth). All measurements are given in mm.

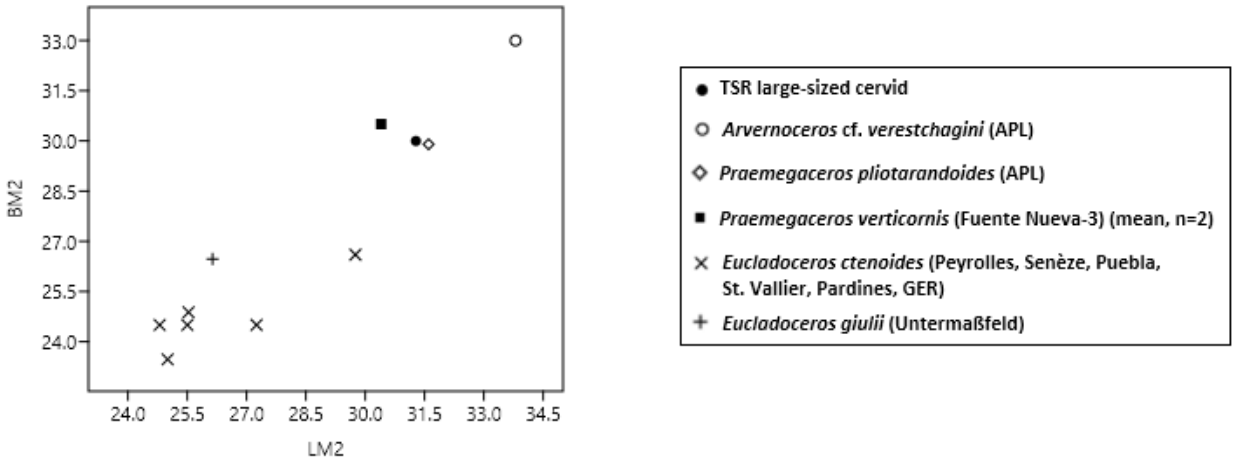

Figure 22. Relative proportions of M2 of large-sized Plio-Pleistocene cervids (L: Length, B: Breadth). All measurements are given in mm.

Morphological observations. In Table 5 we summarize the main differential features between the upper molars of *Praemegaceros* and *Arvernoceros* from APL, *Eucladoceros* and the TSR taxon (Fig. 23).

Arvernoceros cf. *verestchagini* from APL bears upper molars supplemented with entostyles and hypoconal spurs (Croitor & Kostopoulos, 2004). In the TSR cervid, hypoconal spurs are absent, whereas an entostyle is more prominent in M1 and weaker in M2. In *A*. cf. *verestchagini,* the M3 is characterized by small and well-developed cingulum (whereas in M1 and M2 it is absent); in the TSR taxon the cingulum is weak in the upper tooth row.

The upper molars of *Praemegaceros* from APL are advanced: the cingulum is not developed, as in TSR cervid. There is a weak entostyle lingually, similarly to the M2 of the TSR large cervid. The upper tooth row of *Praemegaceros* bears no additional enamel folds/spurs (Croitor & Kostopoulos, 2004); similar to the TSR large-sized cervid. The molars of *Praemegaceros* from APL have a non-cleft lingual wall (as seen mesiodistally); contrarily to the TSR cervid, where the lingual wall, especially of M2, is considerably concave. Such a feature is present in *P. obscurus*, along with hypoconal spurs on the molars (Croitor & Bonifay, 2001; Croitor & Kostopoulos 2004); the latter is absent in the TSR large-sized cervid.

Eucladoceros ctenoides bears upper molars supplemented with protoconal fold (Kostopoulos, 1996) and hypoconal spurs [the posterior wing of the hypocone in all upper molars is bifurcated, forming an eperon (Croitor & Kostopoulos, 2004)]; in sharp contrast to the TSR taxon, where both features are absent. Upper molars are characterized by a well-expressed cingulum which sometimes forms double basal pillars in the TSR large-sized cervid, the cingulum is not particularly developed.

Table 5. Morphological differences between upper molars of P. pliotarandoides*,* A. *cf.* verestchagini *[according to data provided by the material from APL,* E. ctenoides *and TSR large-sized cervid. With (+)/ (-) we symbolize the presence/absence of the feature.*

Dental features/Taxa	*E. ctenoides*	*P. pliotarandoides*	*A.* cf. *verestchagini*	TSR cervid
Hypoconal spurs	+	-	+	-
Protoconal folds	+	-	-	-
Lingual profile (mesiodistal view)	Not concave	Not concave	Concave	Concave
Cingulum	Developed	Not developed	Developed in M3	Not well-developed
Entostyles	+	+ (weak)	+	+

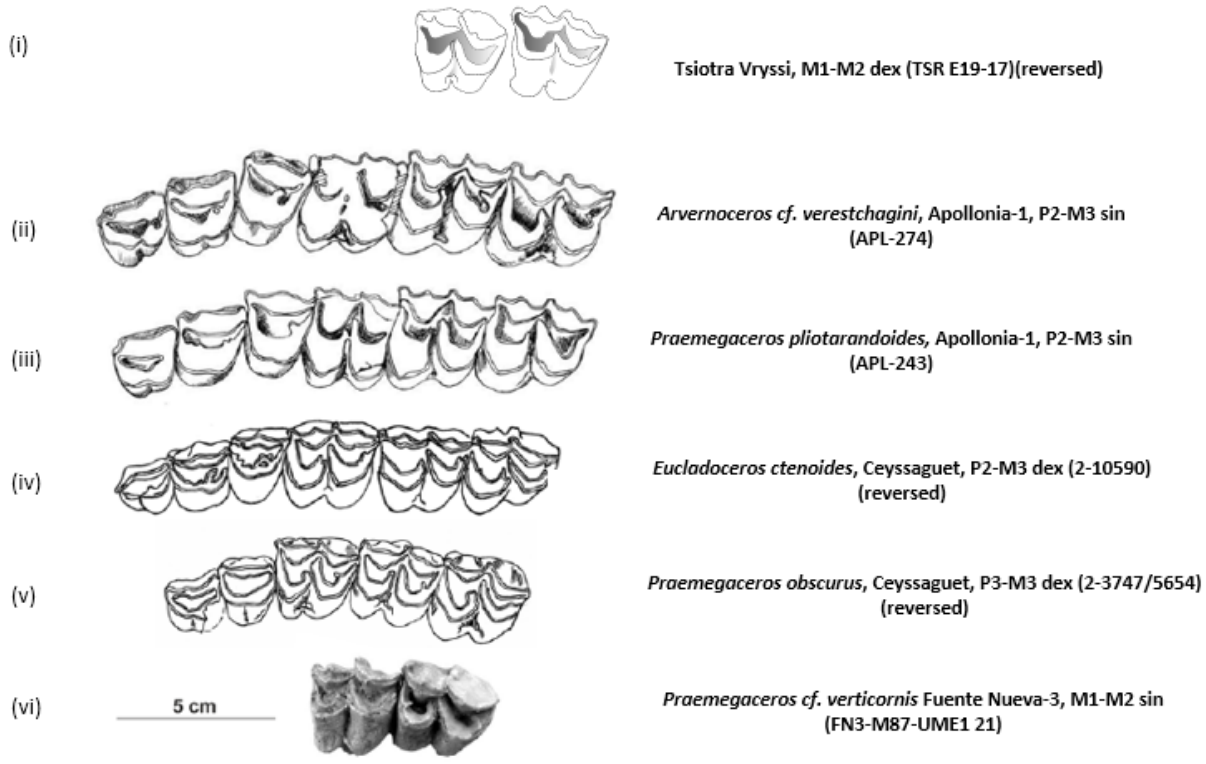

Figure 23. The morphology of upper dentition (occlusal surface) of selected large-sized deer. (ii) and (iii): from Croitor & Kostopoulos (2004), (iv) and (v): from Croitor & Bonifay (2001), (vi): from Abbazzi (2010).

Postcranials. Due to the limited number of specimens (a total of 7 postcranial remains), the attempted metric comparison will focus on the distal part of the tibia of *E. ctenoides* as described by Heintz (1970); *E. ctenoides* from GER (Kostopoulos, 1996); *Eucladoceros* from Oosterschelde (Netherlands) (de Vos et al., 1995); *P. verticornis* as described by Bonifay (1981) and the TSR large-sized cervid (Fig. 24). We also compare the astragali of *Eucladoceros ctenoides*, *Arvernoceros* cf. *verestchagini* and the TSR large-sized cervid (Fig. 25). As shown in Figure 24, the distal end of the tibia from TSR is sharply larger than the one of the several *Eucladoceros* specimens, probably indicating a larger body size for the TSR cervid. *Praemegaceros verticornis* and the TSR cervid share a similar sized distal tibia. The astragalus of *A.* cf. *verestchagini* is larger compared to the TSR taxon, whereas the astragali of the several *Eucladoceros* specimens are close in size to the one from TSR.

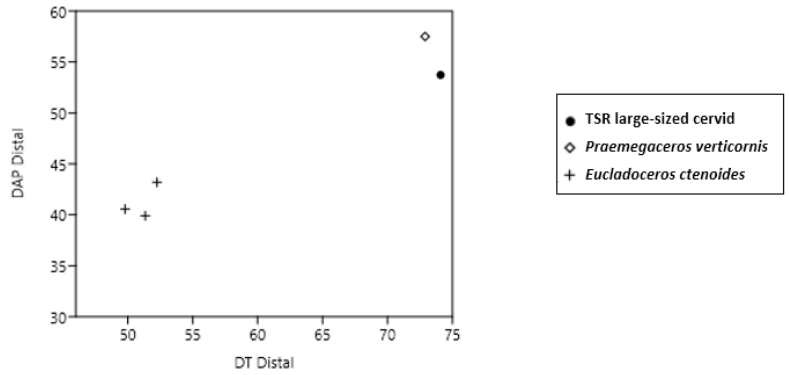

Figure 24. Relative proportions of the distal part of tibias of large-sized European cervids. All measurements are given in mm.

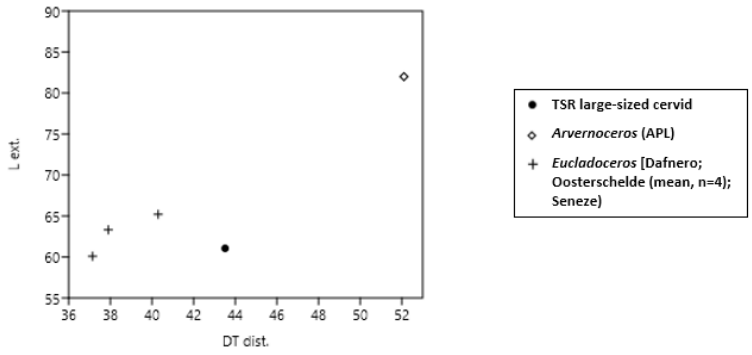

Figure 25. Relative proportions of the astragali of large-sized European cervids. All measurements are given in mm.

4. Discussion

4.1 *Cervus* sp. nov.

Taxonomy. The relative weight of the "small-sized" Plio-Pleistocene European deer is estimated below 100 kg (Croitor, 2006). The small-sized TSR cervid (estimated body mass 75 kg) is of similar size to that of *Metacervocerus rhenanus*, *Metacervocerus. pardinensis* (estimated body mass ~60 kg), *Dama eurygonos* (estimated body mass 70-80 kg) and *Cervus nestii* (estimated body mass of 60-70 kg) (Croitor, 2018, 2019). We exclude from the discussion *D. eurygonos* and later *Dama* taxa due to the sharply differentiated antler morphology, as already stated in the comparison section.

Praeelaphus perrieri is regarded as a medium-sized deer, with a significantly larger size (estimated body mass 180 kg) (Croitor, 2018), compared to TSR small-sized taxon. Considering that the antlers of *P. perrieri* are also larger and of different structure than the studied ones, an attribution to this species is excluded. Nevertheless, it seems that the general antler structure of this genus is quite variable among the different representatives. Table 6 summarizes the comparison of the antler morphology of *Praeelaphus* and the TSR specimen, only in the genus level.

Table 6. Comparison of general antler structure of Praeelaphus *and the TSR cervid.*

Antler features/Taxa	Relative length of pedicle	Number of tines	Orientation of distal fork	Orientation of distal beam compression	Surface of antlers
TSR taxon	Long	4	Sagittal	Sagittal	Ribs, furrows
Praeelaphus	Moderately long	4	Frontal or sagittal	Frontal or sagittal	Ribs, furrows

Among all known contemporaneous taxa, the TSR small cervid shows greatest similarity with *Metacervocerus rhenanus* and *Cervus nesti*. Table 7 summarizes the main antler features of both taxa in comparison to TSR.

Table 7. Main features of antler morphology of TSR taxon, Metacervocerus rhenanus *and* Cervus nestii.

Antler features/Taxa	TSR taxon	*M. rhenanus*	*C. nestii*
Relative length/orientation of pedicle	Long/Posterior	Long/Posterior	Long/Posterior
Number of tines	4	3	4
Orientation of distal fork	Sagittal	Sagittal	Frontal
Orientation of distal beam compression	Sagittal	Sagittal	Frontal
Total length	~600	~710-732 mm	~710 mm
$1^{st} \div 2^{nd}$ segment of the beam	2.5	-	1.6
Deviation of 2^{nd} tine	Medially	-	Laterally
Surface of antlers	Ribs, furrows	Ribs, furrows	Smooth

The antlers of *M. rhenanus* (Fig. 26) and of the TSR cervid share the same sagittal orientation of the distal portion of the antler beam. The antler beam becomes compressed laterally in the part of the distal fork in both taxa. The antler surface is sculptured with longitudinal ribs in both taxa as well. Nevertheless, the first tine of *M. rhenanus'* antlers deviate to the lateral side, whereas in the TSR taxon, a medial deviation is observed.

The main similarity between the TSR small-sized cervid and *C. nestii*'s antlers (Fig. 27) is the presence of four tines in both taxa. Nevertheless, we point out the sharp contrast between the sagittal and the frontal orientation of the beam and the distal bifurcation, in the two cervids respectively.

In addition, in the case of the TSR taxon, the first segment of the beam is significantly longer that the second segment (320:138), whereas in *C. nestii*, the first segment is slightly longer than the second [350mm:220mm; Azzaroli (1992)]. Also, in the TSR taxon, the second tine which is oriented in the parasagittal plane, deviates to the medial side; in contrast to the *C. nestii*'s second tine which deviates to the lateral side.

Figure 26. Antler (dex) of TSR small-sized cervid (a: external side, b: internal side); Antler (sin) of M. rhenanus *from Ceyssaguet (c: external side, b: internal side) (Croitor and Bonifay, 2001).*

Figure 27. (A) Frontal view of the antlers of TSR small-sized cervid, (B) Frontal view of the antlers of C. nestii *from Upper Valdarno (modified from Croitor, 2018), (C) External view of the right antler of TSR cervid, (D) Internal view of the left antler of* Cervus abesalomi *KAHLKE, 2001 (=* C. nestii; *Croitor, 2018) from Dmanisi, modified from Croitor (2006).*

The main dental features of the mentioned cervids are quoted in Table 8. In general, the morphology of premolars in ruminants is highly associated with dietary adaptions. Molarized premolars (physiologically functioning as molars) and shortened premolar series (increasing the molar grinding surface) are both features related to tougher grasses feeding (Spencer, 1995).

Table 8. Main features of dental morphology of the TSR taxon, M. rhenanus and C. nestii.

Features/ Taxa	Development of cingulum (upper toothrow)	Additional enamel folds (upper toothrow)	Premolar/molar ratio Upper/Lower dentition		State of p4 molarization
TSR taxon	Strong	Hypoconal spur in molars	77.2% (n=2)	62% (n=1)	Advanced
M. rhenanus	Weak or absent	Protoconal fold & Hypoconal spur	74% (n=4)	63.5% (n=7)	Primitive
C. nestii	Weak	Absent	74% (n=1)	64.3% (n=1)	Primitive

As evidenced, the small-sized cervid from TSR differs from both *M. rhenanus* and *C. nestii* in the more advanced p4 and the stronger cingulum on the upper molars, though it is characterized by a similarly shortened premolar row.

Considering all available data, we suggest that the TSR-small sized cervid is assigned to a new species, mainly due to its sharply differentiated antler structure, compared to several known Plio-Pleistocene deer of Europe. The genus attribution of the TSR small-sized deer largely depends on the taxonomic scheme followed. Therefore, several alternative views are likely:

(a) If the genus *Cervus* includes *Metacervocerus pardinensis* and *Metacervocerus rhenanus*, as proposed by De Vos et al. (1995), then the number of tines and the orientation of the beam would be regarded as variable characters in the lineage of Plio-Pleistocene *Cervus*. Hence, the TSR taxon could be seen as *Cervus* sp. nov. The attribution of the TSR taxon to *Cervus sensu* Croitor (2018), would also suggest that particularly the orientation of the beam and tines is a variable character in the genus level. As stated by Croitor (2019), the parasagittal crown of modern *C. elaphus* is considered as an evolved character, compared to the transversally oriented distal fork of primitive reprenatatives of *Cervus,* e.g., *C. elaphus acoronatus* and *C. elaphus bactrianus*. If we consider this pattern as an analogue for small-sized cervids as well, we could hypothesize that the TSR species is a relatively advanced Early Pleistocene representative within the

Cervus lineage. According to Croitor (2018), the simple transversal distal fork appeared relatively early in the evolution of the *Cervus* linage (e.g., in *C. nestii*). Hereby, in this study, the small-sized deer from TSR is regarded as a new, relatively advanced species included in the genus *Cervus*.

(b) If *Metacervocerus* is as a valid genus as proposed by Croitor (2018) including cervids of three-pointed antlers, then the TSR cervid would be excluded from it (based on the 4-tines antlers). Nevertheless, it could be equally regarded as a more derived representative, combining certain advanced features (as the occurrence of a fourth tine). In this case however, a revision of the genus would be necessary.

Ecomorphology. The Ruminantia have developed certain ecomorphological adaptation based on the different habitats they inhabit (Köhler, 1993). More specifically, the morphology of the metapodials and phalanges indicate the way the fingers operate in the different ecological niches.

Based on the proximal and the distal part of the metapodials, three main types were suggested (Köhler, 1993): type A1 which corresponds to wooded and moderately humid habitats; type A2 which corresponds to wooded and humid/semiaquatic habitats; type B which indicates open, flat and dry habitats and type C, which indicates mountainous habitats (Fig. 28).

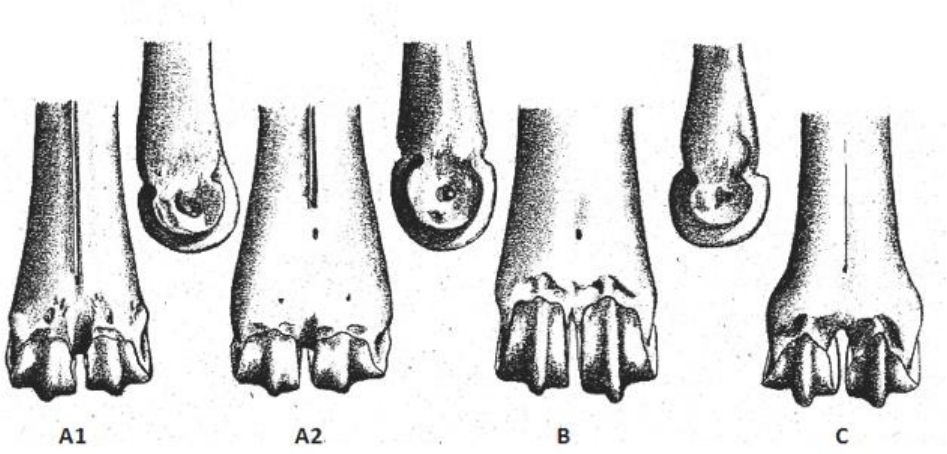

*Figure 28. Distal part of the metacarpus type A1 (*Dama), *A2* (Axis), *B* (Gazella), *C* (Capra). *From Köhler (1993).*

The metatarsals of *Cervus* sp. nov. from TSR correspond with type A2, mainly due to the inflation of the distal part above the low articular surfaces. In Figure 29 we illustrate the metapodials of the TSR *Cervus*, compared to those of *M. rhenanus* (wooded forests), *D. eurygonos* (open and dry landscapes) and *C. nestii* (mountainous habitats) (Croitor, 2006).

Similarity between the metapodial structure of the TSR cervid and *M. rhenanus* is indicated: the part above the distal trochlea is relatively inflated. In the case of *C. nestii*, the metatarsal is relatively short, compared to those of TSR cervid and *D. eurygonos*. The distal part is increasingly broad in a more abrupt way, and the intertrochlear incision forms relatively broader "V", overall showing an affinity with type C. The metatarsal of *D. eurygonos* is relatively longer and the distal articular surfaces are higher and slightly separated. Overall, the thickness of the bone does not alter significantly, mainly resembling type B.

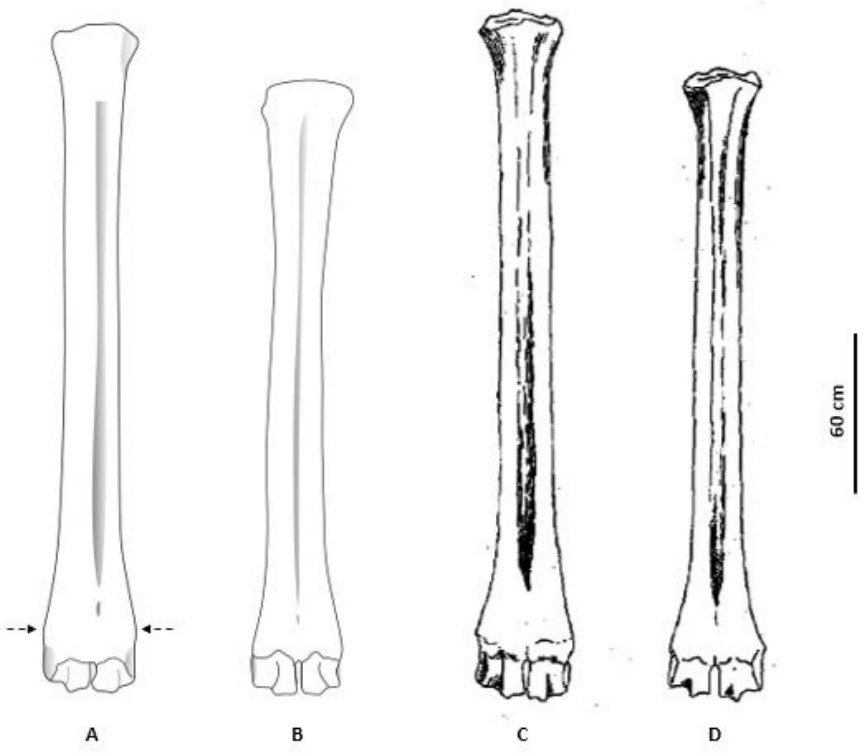

Figure 29. Metapodials (frontal view) of selected small-sized cervids. (A): Metatarsal of Cervus *sp. nov. from TSR, (B) Metacarpal of* M. rhenanus*, (C) Metatarsal of* Dama eurygonos*, (D) Metatarsal of* Cervus nestii*. (C) and (D) are modified from Croitor (2006). The arrows indicate the part above the distal articular surface.*

As shown in Figure 30, there are three main patterns of possible lateral movements of the phalanges. Type A corresponds to moist grounds (enabling lateral movement), type B corresponds to dry ground (rigid in lateral movements), whereas type C is mostly observed in mountain inhabitants (splayed position) (Köhler, 1993).

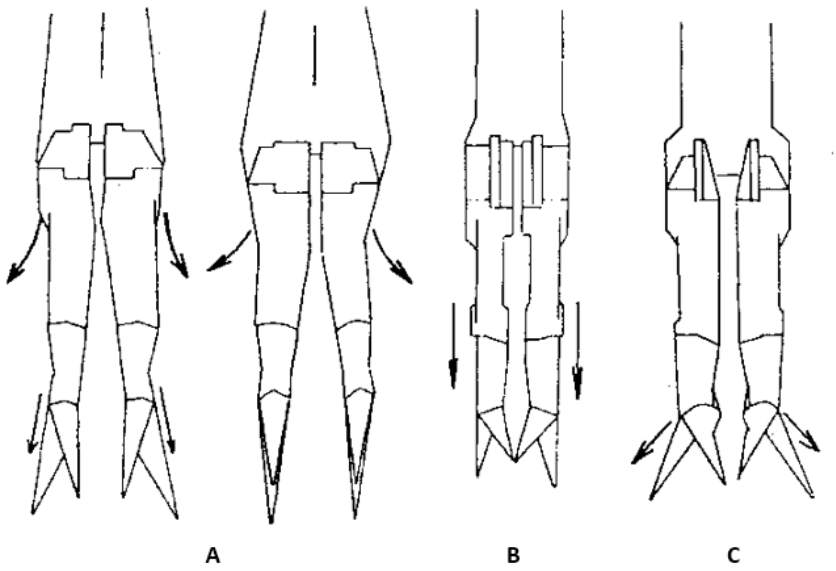

Figure 30. Possible lateral movements of the phalanges in type A, B and C. From Köhler (1993).

The proximal phalanges of the TSR *Cervus* combine certain features of type A and type B. The medial phalanges are also in intermediate state between the A and B type, whereas the distal phalanges display mainly features of type A.

Considering the above, we suggest that the TSR cervid was most probably an inhabitant of a wooded and relatively humid ecological niche. Nevertheless, a detailed geometric morphometric analysis of specific postcranial specimen (e.g., calcaneum, tibia, phalanges) is required, in order to safely assume the exact type of the palaeohabitat, which are particularly variable among cervids (Curran, 2012).

4.2 *Praemegaceros* sp.

Based mainly on the dentition morphology, along with some metric data, we suggest that the large-sized deer from TSR is assigned to the genus *Praemegaceros.* An attribution to species cannot be safely assumed, because the collection is poor (a total of 8 specimens). Nevertheless, the morphology of the upper molars presents an affinity to *P. pliotarandoides/verticornis*, and it clearly distinguishes the TSR cervid from *A.* cf. *verestchagini*, along with *Eucladoceros* representatives.

In terms of ecomorphology, the general structure of the phalanges of *Praemegaceros* from TSR (Fig. 31), resemble the type A, as described by Köhler (1993). More specifically, the proximal phalanges mainly resemble the phalanges of type A (with a slight overlap to Type B), whereas the intermediate and the distal phalanges belong to type A.

As discussed above, phalanges of type A correspond to humid wooded habitats with moist and soft ground. Nevertheless, a detailed approach of the paleoenvironmental conditions would require a relative abundance of teeth specimen, along with antlers, because it is generally accepted that their architecture is an adaptable feature, depending on the density of each habitat (Bubenik & Bubenik, 1990).

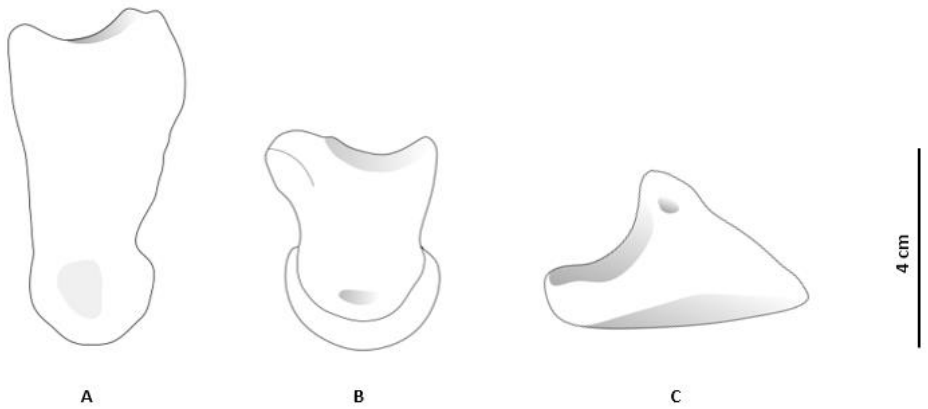

Figure 31. Illustration of the phalanges of Praemegaceros *sp. from TSR. (A) Phalanx I – interdigital side, (B) Phalanx II – external side, (C) Phalanx III – interdigital side.*

4.3 Ecology and Biochronology

Small sized Plio-Pleistocene cervids. The Villafranchian deer of Europe correspond to various types of habitats. *Metacervocerus rhenanus* is an Early Pleistocene species known from faunal assemblages of Spain, France, Netherlands and Greece. The oldest representative of *M. rhenanus* is reported from Saint-Vallier (France), at 2.5 Ma, whereas the earliest remains are reported from Vallonnet (France), at 0.9 Ma (Croitor, 2018).

Certain features, such as the length of the braincase, the long pedicles and the feeding ecology are similar to those of the modern genus *Axis* (Croitor, 2006). Mesowear analysis on the dentition of *M. rhenanus* from Ceyssaguet indicated an ecology similar to modern African bovids (e.g., *Redunca redunca*) that inhabit areas near rivers, with a diet consisting up to 80% of grass. Most probably *M. rhenanus* was an inhabitant of wooded forests (Kaiser & Croitor, 2004) and, unlike *Axis*, underwent notable seasonal alterations (Croitor, 2006).

Cervus nestii is reported from the Early Pleistocene of Italy (Upper Valdarno) and Georgia (Dmanisi; attributed also to *C. abesalomi*). The cranial morphology indicates that *C. nestii* is much closely related to *C. elaphus* than to *C. nippon,* and it is regarded among the most primitive representatives of the "*elaphus* group" (Croitor, 2018). This species is considered mainly as mountain inhabitant, due to the broad epiphyses of long limb bones, the relatively short metapodials and the long robust phalanges (Croitor, 2006). Both cranial and dental features of *C. nestii*, support a browsing feeding.

Dama eurygonos is mainly known from the Villafranchian deposits of Italy (Upper Valdarno). In the fallow deer lineage (*D. eurygonos – D. e. farnetensis – D. vallonnetensis*), the length of the metapodials is progressively increasing and the antlers tend to simplify. These changes indicate gradual adaptations in dry open habitats (Croitor, 2006).

Overall, *Cervus* sp. nov. from TSR probably falls within the ecological niche of *M. rhenanus*. This is supported by the affinity of these taxa in metapodial structure, contrarily to *C. nestii* and fallow deer, as discussed.

Large sized Plio-Pleistocene cervids. As aforementioned, *Eucladoceros* and *Praemegaceros* are regarded as two closely related genera (Vislobokova, 2013), the divergence of which took place at about 2.5 Ma. The early members of *Praemegaceros* appeared during the Early Pleistocene (2.0 Ma) in Inner Asia and were replaced by *P. verticornis* at about 1.2 Ma. *Praemegaceros pliotarandoides* is regarded a synonym to *P. verticornis* by some authors (Kahlke, 1956; Vislobokova, 2012), whereas others regard the former as a probable direct forerunner of the latter (Croitor & Kostopoulos, 2004). *Praemegaceros obscurus* and *P. pliotarandoides* are two closely related species (based on the antler morphology; Croitor, 2018). The genus distributed widely at 0.8 Ma, and its last representatives are known from Apennine Peninsula, at about 366-358 ka (Vislobokova, 2011). The initial evolution of *Praemegaceros* took place in the dry continental climatic conditions of Asia, resulting in more advanced specializations of the antlers and dentaries, as well as a larger body mass, compared to *Eucladoceros.* The latter, remained in regions with temperate climate, and maintained relatively primitive antler and dentition morphology (Croitor, 2009).

Arvernoceros is a genus known from the middle Pliocene-Early Pleistocene of Europe. Its earliest representative is traced at the middle Pliocene of France and Spain, whereas its latest members are reported from the Early Pleistocene of Transcaucasia, Moldova and Greece (David, 1992; Baigusheva, 1994; Croitor & Kostopoulos, 2004). *Arvernoceros* cf. *verestchagini* from the late Villafranchian of Apollonia-1 is an exceedingly large-sized (estimated body mass of 700 kg) (Croitor, 2018) and high-level browser cervid (Croitor & Kostopoulos, 2004). The evolution of *Arvernoceros* during the Pleistocene was linked with increased body weight and complicated antlers, under progressive aridification of the climate and gradual expansion of steppe ecotypes (Baygusheva & Titov, 2013).

In general, the dispersal of megacerines during the Pleistocene was highly associated with the climatic changes. The different biomes, caused by the alternating of cold and warm intervals, played a significant role in the migrations of giant deer (Vislobokova, 2011). As shown in Figure 32, *Praemegaceros* appeared in Eastern Europe at approximately 1.8 Ma. Its representatives are mainly regarded forest-steppe inhabitants, whereas at the interval between 2.0 and 1.0 Ma, thin broad-leaved forests were their most probable biome (Vislobokova, 2011). As mentioned, *Praemegaceros* sp. from TSR is probably associated with humid, wooded forest ecotypes, which comes in agreement with the aforementioned. An opportunistic mixed feeding, highly associated with an increase of glacial cycle amplitude after 1.8-1.6 Ma, is suggested for *Praemegaceros* (Kaiser & Croitor, 2004). During the Early Pleistocene, this dietary adaptation was advantageous over the more specialized feeders (Brugal & Croitor, 2007).

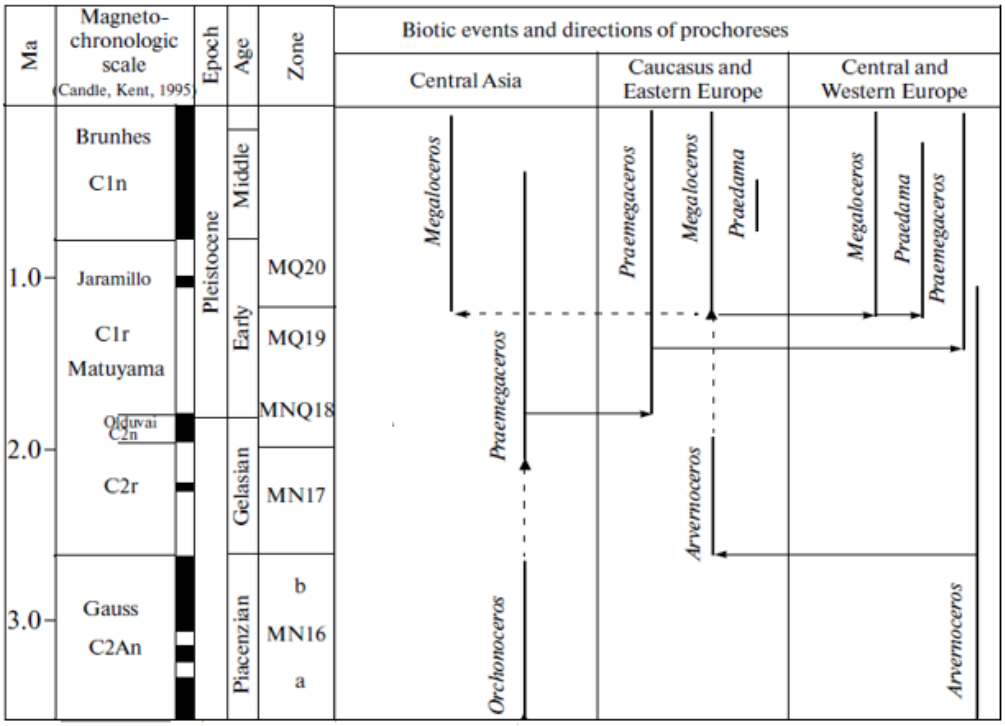

Figure 32. The major events in the history of selected megacerines. Modified from Vislobokova (2012).

Villafranchian cervid assemblages of Greece. Several Greek fossiliferous localities (Fig. 33) have provided Villafranchian cervid assemblages. This is the case of the middle Villafranchian fauna of Volakas (VOL; Drama Basin, Eastern Macedonia), which includes the cervids *Eucladoceros ctenoides*, *Metacervocerus rhenanus* and *Croizetoceros ramosus* (Kostopoulos, 1996). The middle Villafranchian fauna of Sesklo (SES; Thessaly), includes the cervids *E. ctenoides* and *C. ramosus* (Athanasiou, 1996). *Eucladoceros* sp. is described from Reghínio (REG; Phthiotis, Central Greece), dated to the Early Pleistocene, and perhaps correlated to the middle Villafranchian as well (Athanasiou, 2006). The fauna of Dafnero (DFN; Aliakmon Basin, Western Macedonia), correlated to the middle Villafranchian (Koufos, 2014), yielded the cervids *E. ctenoides* and *M. rhenanus* (Kostopoulos, 1996). The fauna of Gerakarou-1 (GER; Mygdonia basin), correlated the middle/late Villafranchian boundary (Koufos, 2014), includes the cervids *E.* cf. *ctenoides*, *Metacervocerus* sp. and *C. ramosus gerakarensis* (Kostopoulos, 1996).

The late Villafranchian fauna of Apollonia-1 (APL; Mygdonia basin), includes *Praemegaceros pliotarandoides* and *Arvernoceros* cf. *verestchagini* (Croitor & Kostopoulos, 2004). The fauna of Libakos (LIB; Aliakmon Basin, Western Macedonia), correlated to the late Villafranchian as well (Gkeme et al., 2017), yielded *Megaloceros* aff. *savini* (van der Made, 2015), here mentioned as *Praedama* aff. *savini* [Koufos & Kostopoulos (2016); Croitor (2018)] and *Dama vallonnetensis* (Kostopoulos pers. com). Finally, the late Villafranchian faunas of Kalamoto (KLT & KAL; Mygdonia Basin), include the cervids *Praemegaceros pliotarandoides*, *Cervus* sp. and *Dama* sp. (Tsoukala & Chatzopoulou, 2005)

It has to be noted, that the localities of Gerakarou-1, Apollonia-1 and Kalamoto are within the Mygdonia basin and thus geographically very close to Tsiotra Vryssi. The fauna of Tsiotra Vryssi is of intermediate age between Gerakarou-1 and Apollonia-1, and close in age with the Libakos one (1.8-1.2 Ma).

Figure 33. Map of Greece, indicating certain Plio-Pleistocene fossiliferous localities with cervid remains.

Summing up, the middle Villafranchian cervid assemblages of Greece mainly consist of the genera *Croizetoceros* – *Metacervocerus* – *Eucladoceros.* This association is also typical of several other Villafranchian deposits of Western Europe, e.g., Perrier, Coupet, Chilhac, Senèze, Saint Vallier (France), La Puebla de Valverde (Spain) (Heintz, 1970) and Fonelas P-1 (Spain) (Garrido, 2008). Moving towards the late Villafranchian, an alteration in this typical cervid association is observed, accompanied by a disappearance of the mentioned taxa. The late Villafranchian faunas of Greece consist of the relatively well-represented genus *Praemegaceros*, along with members of *Dama*, *Cervus*, *Praedama* and *Arvernoceros*.

The affinities between *Metacervocerus rhenanus* and *Cervus* sp. nov. from TSR are thus far discussed. The absence of the former from the perhaps isochronous faunas of TSR

and LIB, along with the slightly younger fauna of APL, might indicate the disappearance or replacement of this cervid, by another, more advanced form. *Praedama* aff. *savini* from LIB combines primitive mandibular and dental features, and it is regarded among the oldest known representatives of this genus in Europe (van der Made, 2008). Remains of *Dama vallonnetensis* are mostly known from the Epivillafranchian of Vallonnet (France), along with the late Villafranchian of Pirro Nord (Italy) (Croitor, 2018). The presence of the mentioned cervids in the fauna of LIB is part of an advanced late Villafranchian faunal assemblage (Gkeme, 2016).

Croizetoceros ramosus is well represented in middle Villafranchian localities of Greece, and generally in the European Mediterranean region. The extinction of this species took place soon after the "*Pachycrocuta* event" (Croitor, 2018). Its absence from the faunal assemblages of TSR, LIB and APL is in agreement with the correlation of these sites to the late Villafranchian.

Overall, the majority of the middle and middle/late Villafranchian faunal assemblages of Greece (VOL, DFN, SES and GER) include large-sized cervids attributed to the genus *Eucladoceros*, with the representative from GER being more advanced than the other forms (Kostopoulos & Athanassiou, 2005). This genus is absent from the TSR, LIB, APL and other late Villafranchian faunas. *Eucladoceros ctenoides* probably disappeared from Greece close to the "*Pachyrcocuta* event" (Croitor & Brugal, 2007). In Europe, *E. dicranios* is gradually replaced by the much larger *Praemegaceros obscurus*.

Both TSR and APL yielded representatives of the genus *Praemegaceros*. The dispersal of *Praemegaceros* from Eastern to Western Palearctic is part of the significant faunal turnover during the beginning and the middle part of the late Villafranchian (approximately at 1.9-1.7 Ma) (Vislobokova 2016). The oldest known remains of *Praemegaceros* in Europe are reported from the late Villafranchian fauna of Trlica (TRL 11-10) (Montenegro), at 1.8-1.2 Ma (Vislobokova, 2016). The first occurence of *Praemegaceros* in Greece, took place also during the late Villafranchian, signaled first in the older TSR (perhaps roughly contermpronaeous with Trlica 11-10), and subsequently in the younger APL fauna.

We point-out the gradual increase in the body mass of cervids, and generally in ungulates, that reaches its maximum during the Middle Pleistocene (Croitor & Brugal, 2007). The growth in body mass is associated with lower metabolic rates, in order for the ruminants to survive under lower quality nutrition of higher cellulose content (Janis, 1976), linked with a progressive aridification of the climate in the Mediterranean during the Middle Pleistocene (Croitor & Brugal, 2007). In Greece, such an alteration is supported by the presence of large-sized members of *Praemegaceros,* along with the excessively large-sized *Arvernoceros* from APL. Adaptations in arid environmental conditions are also demonstrated in certain cranial features of *Dama vallonnetensis* (Croitor, 2018), a cervid which, as previously mentioned, is present in the late Villafranchian of Greece.

5. Conclusions

Using both metrical and morphological data, the small-sized cervid from TSR, with an estimated body mass of 75 kg, is provisionally assigned to *Cervus* sp. nov., mainly due to the significantly differentiated morphology of the antler structure that distinguishes this species from other Plio-Pleistocene European representatives of similar size. It is suggested that this cervid inhabited relatively humid and wooded ecotypes, based on the metapodial and phalangeal morphology.

Cervus sp. nov. shares certain similarities in antler structure with both *Cervus nestii* and *Metacervocerus rhenanus.* In terms of dental morphology, a closer affinity with *M. rhenanus* is indicated. The structure of the metapodials also support a similar ecological niche for both *M. rhenanus* and *Cervus* sp. nov.

The genus attribution primarily depends on the grounds that *Cervus* and *Metacervocerus* represent two different valid genera, as proposed by the taxonomic scheme followed (Croitor, 2018). On the contrary, previous authors (Heintz 1970; de Vos, 1995) attributed the representatives of *Metacervocerus* (*rhenanus/pardinensis)* to the genus *Cervus*. Thus, a future investigation of the relative significance of the diagnostic features that may indeed distinguish these genera, is required.

The large-sized deer has an estimated body mass of 465 kg, and it is attributed to *Praemegaceros* sp. Further taxonomic identification could not be conducted, due to the scarcity of the available specimens. Its phalangeal morphology indicates a relatively humid and wooded landscape; further material and palaeoecological evidence is needed to support this observation. If new data confirm the present results, *Praemegaceros* from TSR is the oldest known representative of the genus in Greece.

The Greek middle Villafranchian localities include the typical assemblage of *Croizetoceros – Metacervocerus – Eucladoceros*. The fauna of TSR along with the roughly contemporaneous fauna of LIB and the younger fauna of APL, are characterized by the absence of these taxa, due to the significant faunal turnover during the late Villafranchian.

References

Abbazzi, L., 2010. La fauna de cérvidos de Barranco León y Fuente Nueva-3, in: Toro, I., Martínez Navarro, B., Agustí, J. (Eds.), Ocupaciones humanas en el Pleistoceno Inferior y Medio de la Cuenca de Guadix-Baza. Consejería de Cultura, Junta de Andalucía, Arqueología Monografías, Sevilla, 273-290.

Athanassiou, A., 1996. Contribution to the study of the fossil mammals of Thessaly, Greece. PhD thesis, National and Kapodistrian University of Athens, Athens, pp. 1-393 (in Greek).

Athanassiou, A., 2006. Reghinio, a new mammal locality from the Plio-Pleistocene of Central Greece. Neues Jahrbuch für Geologie und Paläontologie-Monatshefte, 116-128.

Azanza, B., Rössner, G. E., Ortiz-Jaureguizar, E., 2013. The early Turolian (late Miocene) Cervidae (Artiodactyla, Mammalia) from the fossil site of Dorn-Dürkheim 1 (Germany) and implications on the origin of crown cervids. Palaeobiodiversity and Palaeoenvironments, 93, 217-258.

Azzaroli, A., 1947. I cervi fossili della Toscana. Palaeontographia Italica, 43, 46-81.

Azzaroli, A., 1992. The cervid genus *Pseudodama* n. g. in the Villafranchian of Tuscany. Palaeontographia Italica, 79, 1-41.

Baygusheva, V.S., 1994. On skull construction of the large-sized deer of the Khaprovian mammal assemblage. Paleoteriologia, 236-252 (in Russian).

Baygusheva, V. S., Titov, V. V., 2013. Large deer from the Villafranchian of Eastern Europe (Sea of Azov Region): evolution and paleoecology. Quaternary international, 284, 110-122.

Bonifay, M. F., 1981. Les Praemegaceros du Pléistocène moyen de la grotte de l'Escale à Saint-Estève-Janson (Bouches-du-Rhône). Leur intérêt dans le contexte biostratigraphique européen. Quaternaire, 18, 109-120.

Brooke, V., 1878. On the classification of the Cervidae with the synopsis of the existing species. Proceedings of the Zoological Society of London 46, 883-928

Bubenik, G. A., Bubenik, A. B., 2012. Horns, pronghorns, and antlers: evolution, morphology, physiology, and social significance. Springer Science & Business Media. pp. 1-562.

Cap, H., Aulagnier, S., Deleporte, P., 2002. The phylogeny and behaviour of Cervidae (Ruminantia Pecora). Ethology Ecology & Evolution, 14, 199-216.

Cronin, M. A., 1991. Mitochondrial-DNA phylogeny of deer (Cervidae). Journal of Mammalogy, 72, 553-566.

Croitor, R. V., 2001. Functional morphology of small-sized deer from the Early and Middle Pleistocene of Italy: implication for paleolandscape reconstruction. The World of Elephants: 1st International Congress, Rome.

Croitor, R., 2006a. Early Pleistocene small-sized deer of Europe. Hellenic Journal of Geosciences, 41, 89-117.

Croitor, R., 2006b. Taxonomy and systematics of large-sized deer of the genus *Praemegaceros* Portis, 1920 (Cervidae, Mammalia). In: R.D. Kahlke, L.C. Maul, P.P.A. Mazza (Eds), Late Neogene and Quaternary biodiversity and evolution: Regional developments and interregional correlations. Volume I. Courier Forschungsinstitut Senckenberg 256, 91-116.

Croitor, R., 2009. Phylogeny and speciation in Quaternary cervid genera *Eucladoceros* and *Praemegaceros* (Cervidae, Mammalia). In Seventh Romanian Symposium on Palaeontology (p. 29).

Croitor, R., 2011. A skull of *Praemegaceros pliotarandoides* (Cervidae, Mammalia) from the Taman Peninsula (South-West Russia). Acta Palaeontologica Romaniae, 7, 113-121.

Croitor, R., 2012. Lower Pleistocene ruminants from Monte Riccio (Tarquinia, Italy). Oltenia. Studii şi conumicări. Ştiinţele naturii, 28, 221-226.

Croitor, R., 2017. Description of a new deer species (Cervidae, Mammalia) from the Early Pliocene of Eastern Europe, with a review of early dispersals and palaeobiogeography of the subfamily Cervinae. Neues Jahrbuch für Geologie und Paläontologie-Abhandlungen, 283, 85-108.

Croitor, R., 2018. Plio-Pleistocene deer of Western Palearctic: Taxonomy, systematics, phylogeny. Academy of Sciences of Moldova, Chişinău, pp. 1-140.

Croitor, R., 2019. A new form of wapiti *Cervus canadensis* Erxleben, 1777 (Cervidae, Mammalia) from the Late Pleistocene of France, Palaeoworld, doi: https://doi.org/10.1016/j.palwor.2019.12.001

Croitor, R., Bonifay M.-F., 2001. Étude préliminaire des cerfs du gisement Pleistocène inférieur de Ceyssaguet (Haut-Loire). Paleo, 13, 129-144.

Croitor, R., Kostopoulos D. S., 2004. On the systematic position of the large-sized deer from Apollonia, Early Pleistocene, Greece. Paläontologische Zeitschrift, 78, 137-159.

Croitor, R., & Brugal, J., 2007. New insights concerning Early Pleistocene cervids and bovids in Europe: dispersal and correlation. Courier Forschungsinstitut Senckenberg, 259, 47.

Curran, S. C., 2012. Expanding ecomorphological methods: geometric morphometric analysis of Cervidae post-crania. Journal of Archaeological Science, 39, 1172-1182.

Curran, S. C., 2015. Exploring *Eucladoceros* ecomorphology using geometric morphometrics. The Anatomical Record, 298, 291-313.

David, A., 1992. A new deer species (Cervidae, Mammalia) from the late Pliocene deposits of Moldova (in Russian). Buletinul Academiei de Ştiinţe din Republica Moldova. Seria Ştiinţelor Chimice şi Biologice, 1, 67-68.

Davis, L. B., 2010. Precontact Archaeology and Prehistory of the Central Montana High Plains (No. 5). BLM, Montana State Office. pp. 1-292.

Di Stefano, G., Petronio, C., 2002. Systematics and evolution of the Eurasian Plio-Pleistocene tribe Cervini (Artiodactyla, Mammalia). Geologica Romana, 36, 311-334.

Fernández, M. H., Vrba, E. S., 2005. A complete estimate of the phylogenetic relationships in Ruminantia: a dated species-level supertree of the extant ruminants. Biological reviews, 80, 269-302.

Garrido, G., 2008. La asociación de los géneros *Croizetoceros, Metacervoceros* y *Eucladoceros* (Cervidae, Artiodactyla, Mammalia) en el yacimiento de Fonelas P-1 (Cuenca de Guadix, Granada). Vertebrados del Plioceno superior terminal en el suroeste de Europa: Fonelas P-1 y el Proyecto Fonelas. Cuadernos del Museo Geominero, 10, 365-396.

Geist V., 1998. Deer of the World: Their Evolution, Behaviour, and Ecology. Mechanicsburg, PA: Stackpole Books, pp. 1-421.

Gentry, A. W., Rössner, G. E., Heizmann, E. P. J., 1999. Suborder Ruminantia. The Miocene Land Mammals of Europe. München. 225-258.

Gilbert, C., Ropiquet, A., Hassanin, A., 2006. Mitochondrial and nuclear phylogenies of Cervidae (Mammalia, Ruminantia): systematics, morphology, and biogeography. Molecular phylogenetics and evolution, 40, 101-117.

Giusti, D., Konidaris, G. E., Tourloukis, V., Marini, M., Maron, M., Zerboni, A., Thompson, N., Koufos, G. D., Kostopoulos, D. S., Harvati, K., 2019. Recursive anisotropy: a spatial taphonomic study of the Early Pleistocene vertebrate assemblage of Tsiotra Vryssi, Mygdonia Basin, Greece. Boreas, 48, 713–730.

Gkeme, A., 2016. Study of the Pleistocene equids of the Eltgen collection (localities Livakos, Kapetanios, Polylakkos, W. Macedonia). Master's thesis, Aristotle University of Thessaloniki. pp. 1-169

Gkeme, A., Koufos, G. D., Kostopoulos, D. S., 2017. The Early Pleistocene stenonoid horse from Libakos (Western Macedonia, Greece): Biochronological and palaeoecological implications and dispersal events. In 15th RCMNS Congress (Athens).

Grubb, P., 2000. Valid and invalid nomenclature of living and fossil deer. Acta Theriologica 45, 289-307.

Hammer, Ø., Harper, D.A.T., Ryan, P.D., 2001. PAST: Paleontological statistics software package for education and data analysis. Palaeontologia Electronica 4, 9.

Hassanin, A., Delsuc, F., Ropiquet, A., Hammer, C., Van Vuuren, B. J., Matthee, C., Ruiz-Garcia, M., Catzeflis, F., Areskoug, V., Nguyen, T.T., Couloux, A., 2012. Pattern and timing of diversification of Cetartiodactyla (Mammalia, Laurasiatheria), as revealed by a comprehensive analysis of mitochondrial genomes. Comptes rendus biologies, 335, 32-50.

Heckeberg, N. S., Wörheide, G., 2019. A comprehensive approach towards the systematics of Cervidae (No. e27618v1). PeerJ Preprints.

Heintz E., 1970. Les cervidés villafranchiens de France et d'Espagne. Mémoires du Muséum national d'histoire naturelle. Série C, Sciences de la terre, 22, 1-303 + Figures et tableaux, pp. 1-206.

Hillson, S., 2016. Mammal bones and teeth: an introductory guide to methods of identification. Routledge. pp. 1-132.

Janis, C., 1976. The evolutionary strategy of the Equidae and the origins of rumen and cecal digestion. Evolution, 30, 757-774.

Janis, C. M., 1990. Correlation of cranial and dental variables with body size in ungulates and macropodoids. In: Damuth, J. and MacFadden, B. J. (Eds.), Body Size in Mammalian Paleobiology: Estimation and Biological Implications. Cambridge University Press, Cambridge, pp. 255-299.

Kahlke, H.-D., 1956. Die Cervidenreste aus den altpleistozänen Ilmkiesen von Süßenborn bei Weimar. Akademie Verlag, I-III, 1-62; Berlin.

Kaiser, T. M., Croitor, R., 2004. Ecological interpretations of early Pleistocene deer (Mammalia, Cervidae) from Ceyssaguet (Haute-Loire, France). Geodiversitas, 26, 661-674.

Kockel, F., Mollat, H., Walther, H.W., 1977. Erläuterungen zur geologischen Karte der Chalkidiki und angrenzender Gebiete 1:100.000 (Nord-Griechenland). Bundesanstalt für Geowissenschaften und Rohstoffe, Hannover, pp. 1-119.

Köhler, M., 1993. Skeleton and habitat of recent and fossil ruminants. Münchner Geowissenschaftliche Abdhandlungen, 25, 1-88.

Konidaris, G. E., Tourloukis, V., Kostopoulos, D. S., Thompson, N., Giusti, D., Michailidis, D., Koufos G. D., Harvati, K., 2015. Two new vertebrate localities from the Early Pleistocene of Mygdonia Basin (Macedonia, Greece): preliminary results. Comptes Rendus Palevol, 14, 353-362.

Konidaris, G. E., Kostopoulos, D. S., Koufos, G.D., Tourloukis, V., Harvati K., 2016 Tsiotra Vryssi: a new vertebrate locality from the Early Pleistocene of Mygdonia Basin (Macedonia, Greece). XIV Annual Meeting of the European Association of Vertebrate Palaeontologists. Haarlem, Koninklijke Nederlandse Akademie Van Wetenschappen.

Kostopoulos, D. S., Athanassiou, A., 2005. In the shadow of bovids: suids, cervids and giraffids from the Plio-Pleistocene of Greece, in: Crégut-Bonnoure, É., (Ed.), Les Ongulés Holarctiques du Pliocène et du Pléistocene. Quaternaire, Hors-Série. 2, 179–190.

Kostopoulos, D. S., Maniakas I., Tsoukala E., 2018. Early bison remains from Mygdonia Basin (Northern Greece). Geodiversitas 40, 283-319.

Kostopoulos, D. S., 1996. The Plio-Pleistocene artiodactyls of Macedonia (Greece); systematics, palaeoecology, biochronology, biostratigraphy. Unpublished PhD Thesis, Aristotle University of Thessaloniki. (In Greek with English summary).

Koufos, G. D., Syrides, G. E., Kostopoulos, D. S., Koliadimou K. K., 1995. Preliminary results about the stratigraphy and the palaeoenvironment of Mygdonia Basin, Macedonia, Greece. Geobios, M.S. 18, 243-249.

Koufos, G. D., Kostopoulos, D. S., 2016. The Plio-Pleistocene large mammal record of Greece: Implications for early human dispersals into Europe. In Paleoanthropology of the Balkans and Anatolia. Springer, Dordrechtpp, 269-280.

Koufos, G. D., Konidaris, G. E., Harvati, K., 2018. Revisiting *Ursus etruscus* (Carnivora, Mammalia) from the Early Pleistocene of Greece with description of new material. Quaternary International, 497, 222-239.

Koufos, G. D., 2014. The Villafranchian carnivoran guild of Greece: implications for the fauna, biochronology and paleoecology. Integrative zoology, 9, 444-460.

Koufos, G. D., 2016. Neogene and Quaternary continental biostratigraphy of Greece based on mammals. Bulletin of the Geological Society of Greece, 50, 55-64.

Koufos, G. D., 2018. New Material and Revision of the Carnivora, Mammalia from the Lower Pleistocene Locality Apollonia 1, Greece. Quaternary, 1, 6.

Kuznetsova, M. V., Kholodova, M. V., Danilkin, A. A., 2005. Molecular phylogeny of deer (Cervidae: Artiodactyla). Russian Journal of Genetics, 41, 742-749.

Maniakas, I., Kostopoulos, D. S., 2017. Morphometric-palaeoecological discrimination between Bison populations of the western Palaearctic. Geobios, 50, 155-171.

Metcalfe, D., Jones, K. T., 1988. A reconsideration of animal body-part utility indices. American Antiquity, 53, 486-504.

Pales, L., Lambert, C., 1971. Atlas ostéologique: pour servir à l'identification des mammifères du Quaternaire. Les membres Herbivores. Centre National de la Recherche Scientifique. pp. 1-181.

Pfeiffer, T., 1999. Die Stellung von *Dama* (Cervidae, Mammalia) im System plesiometacarpaler Hirsche des Pleistozäns - Phylogenetische Rekonstruktion - Metrische Analyse. Courier Forschungsinstitut Senckenberg, 211, 1–218.

Psilovikos, A. A., 1977. Palaeogeographic development of the basin andlake of Mygdonia (Langada-Volvi area), Greece. Aristotle University of Thessaloniki, Thessaloniki, pp. 1-156.

Rook, L., Martínez-Navarro, B., 2010. Villafranchian: the long story of a Plio-Pleistocene European large mammal biochronologic unit. Quaternary International 219, 134–144.

Scott, K. M., 1983. Prediction of body weight of fossil Artiodactyla. Zoological Journal of the Linnean Society, 77, 199-215.

Scott, R. S., 2004. The comparative paleoecology of Late Miocene Eurasian hominoids. Ph.D. Dissertation. The University of Texas at Austin.

Spencer, L., 1995. Morphological correlates of dietary resource partitioning in the African Bovidae. Journal of Mammalogy 76, 448-471.

Tsoukala, E., Chatzopoulou, K., 2005. A new Early Pleistocene (latest Villafranchian) site with mammals in Kalamotó (Mygdonia Basin, Macedonia, Greece) – Preliminary report. Mitt. Komm. Quartärforsch. Österr. Akad. Wiss, 14, 213-233.

van der Made, J., Tong, H. W., 2008. Phylogeny of the giant deer with palmate brow tines *Megaloceros* from west and *Sinomegaceros* from east Eurasia. Quaternary International, 179, 135-162.

van der Made, J., Dimitrijević, V., 2015. *Eucladoceros montenegrensis* n. sp. and other Cervidae from the Lower Pleistocene of Trlica (Montenegro). Quaternary International, 389, 90-118.

Vislobokova, I. A., Agadjanian, A. K., 2016. On the history of Early—Middle Pleistocene mammal faunas of the Central Balkans. Paleontological Journal 50.2, 187-201.

Vislobokova, I. A., 2011. Historical development and geographical distribution of giant deer (Cervidae, Megacerini). Paleontological Journal, 45, 674-688.

Vislobokova, I. A., 2012. Giant deer: Origin, evolution, role in the biosphere. Paleontological Journal, 46, 643-775.

Vislobokova, I. A., 2013. Morphology, taxonomy, and phylogeny of megacerines (Megacerini, Cervidae, Artiodactyla). Paleontological Journal, 47, 833-950.

Von den Driesch, A., 1976. A guide to the measurement of animal bones from archaeological sites. Peabody Museum Press. pp. 1-148.

Vos J. de, Mol D., Reumer, J. W. F., 1995. Early pleistocene Cervidae (Mammalia, Artiodactyla) from the Oosterschelde (the Netherlands), with a revision of the cervid genus *Eucladoceros* Falconer, 1868. Deinsea, 2, 95-121.

Yang, C., Li, P., Zhang, X., Guo, Y., Gao, Y., Xiong, Y., Wang L., Qi W., Yue, B., 2012. The complete mitochondrial genome of the Chinese Sika deer (*Cervus nippon* Temminck, 1838), and phylogenetic analysis among Cervidae, Moschidae and Bovidae. Journal of natural history, 46, 1747-1759.

Appendix I

Table 1. Measurements of the pedicle and burr of the antlers of Cervus *sp. nov. from TSR. L: height, DT: maximum transversal diameter and DAP: maximum antero-posterior diameter. Fragmented material is noted with (-).*

TSR D18-100	Pedicle: Length	Pedicle: DT	Pedicle: DAP	Burr: DT	Burr: DAP
Left antler	24	32.46	30.35	42.34	50.00
Right antler	23.9	29.83	30.89	-	-

Table 2. Measurements of the antlers of Cervus *sp. nov. from TSR. (4) Length of first segment (5) Length of second segment (6) Length of third segment (7) Total length in straight line (8) Total length following the curvatures (9) Length of 1st tine (10) Length of 2nd tine. Fragmented material is noted with (-).*

TSR D18-100	4	5	6	7	8	9	L of post. /ant. tines		Angle of 2nd tine & beam	Distal fork: angle of tines
Left antler	60.53	360	-	>520	>540	>110	-		74°	-
Right antler	55.08	320	138	>600	>660	220	>100	>55	74°	80°

Table 3. Measurements of upper dentition of Cervus *sp. nov. from TSR. L=maximum length, B=maximum breadth. Fragmented material is noted with (-).*

Specimen	LPM	LP	LM	LP2	BP2	LP3	BP3	LP4	BP4	LM1	BM1	LM2	BM2	LM3	BM3
TSR 135	84.79	40.51	50.12	15.51	14.52	12.51	15.90	11.83	16.30	15.75	17.12	18.41	18.37	18.21	18.15
TSR 156	85.65	40.85	54.88	12.85	12.21	12.45	13.09	13.81	13.48	16.61	16.42	20.54	17.09	19.03	13.77
TSR G16-38	-	-	44.57	-		-		11.75	8.75	14.65	11.30	15.02	12.11	17.65	12.52

Table 4. Measurements of lower dentition of Cervus *sp. nov. from TSR. L=maximum length, B=maximum breadth. Fragmented material is noted with (-).*

Dentition	LPM	LP	LM	Lp2	Bp2	Lp3	Bp3	Lp4	Bp4	Lm1	Bm1	Lm2	Bm2	Lm3	Bm3
TSR E13-5	-	-	-	-		12.32	7.99	13.37	8.30	15.42	10.68	18.39	12.29	-	
TSR D18-99	88.02	34.69	54.52	10.44	5.97	11.91	7.51	12.37	8.35	14.84	10.87	17.86	11.57	22.72	10.54
TSR F20-49	-	34.33	-	9.93	5.91	11.46	7.62	12.93	8.72	14.88	10.05	16.87	11.28	-	

Table 5. Measurements of the right mandible of Cervus *sp. nov. from TSR. T.H.: Total height of the mandible. Fragmented material is noted with (-).*

Mandible	4	5	6	7	8	9	10	11	12	13	14	15	T.H.
TSR D18-99	>205.15	>55.79	-	-	51.06	~15.84	25.71	26.42	31.13	9.98	14.15	15.28	109.19

Table 6. Measurements of the humerus of Cervus *sp. nov. from TSR. DT: maximum transversal diameter and DAP: maximum antero-posterior diameter.*

Humerus	DT Distal	DAP Distal
TSR H17-22e	36.08	34.92
TSR D18-107	~37.94	27.12
TSR-149	41.63	38.45

Table 7. Measurements of the radius of Cervus *sp. nov. from TSR. L: maximum length, DT: maximum transversal diameter and DAP: maximum antero-posterior diameter.*

Radius	L	DT diaph.	DAP diaph.	DT prox.	DAP prox.	DT dist.	DAP dist.
TSR H17-22d	152.50	19.63	12.74	31.95	23.71	35.94	18.70

Table 8. Measurements of the metacarpal of Cervus *sp. nov. from TSR. Fragmented material is noted with (-).*

Metacarpal	PAP	PML	MML	MLEN	FLEN	MAP	AVML	DDML	IDML
TSR C16-27	19.91	26.99	-	>130.61	-	-	-	-	-

Table 9. Measurements of the femur of Cervus *sp. nov. from TSR. L: maximum length, DT: maximum transversal diameter and DAP: maximum antero-posterior diameter. Fragmented material is noted with (-).*

Femur	L	DT Diaphysis	DAP Diaphysis	DT Proximal	DAP Proximal	DT Distal	DAP Distal
TSR D18-48	229.65	21.37	22.94	21.20	-	52.23	66.58

Table 10. Measurements of the tibias of Cervus *sp. nov. from TSR. L: maximum length, DT: maximum transversal diameter and DAP: maximum antero-posterior diameter. Fragmented material is noted with (-).*

Tibias	L	DT diaph.	DAP diaph.	DT prox.	DAP prox.	DT dist.	DAP dist.
TSR H17-12	-	-	-	-	-	35.83	27.20
TSR D18-103	-	-	-	-	-	35.68	28.83
TSR D18-84	-	-	-	-	-	36.45	28.12
TSR C18-13	-	-	-	-	-	38.15	28.59
TSR C17-45	-	-	-	-	-	37.79	29.30
TSR-110	-	-	-	-	-	34.04	25.37
TSR D18-50a	295.34	26.24	24.4	63.16	60.23	38.53	29.82

Table 11. Measurements of the astragali of Cervus *sp. nov. from TSR. DT: maximum transversal diameter, DAP: maximum antero-posterior diameter, L ext: length of the external side, L int: length of the internal side. Fragmented material is noted with (-).*

Astragali	DT diaph.	DAP diaph.	DT prox.	DAP prox.	DT dist.	DAP dist.	L ext.	L int.
TSR C18-13	24.94	21.64	-	-	25.20	20.80	40.48	38.32
TSR D18-102	25.06	22.70	24.38	23.58	25.89	19.39	40.69	38.77
TSR D18-83	24.49	22.19	24.17	23.99	25.15	21.11	41.27	38.69
TSR D18-51	22.95	21.00	23.25	21.48	23.86	18.64	38.78	36.59
TSR H17-14a	24.40	21.44	24.68	22..80	24.70	20.2o	39.61	36.67
TSR H17-8b	23.16	20.24	22.97	21.98	24.10	18.96	38.53	35.96
TSR F17-34	23.28	20.86	24.03	24.53	24.11	19.96	38.88	36.61

Table 12. Measurement of the calcanei of Cervus *sp. nov. from TSR. GB: Greatest breadth, GL: Greatest length.*

Calcanei	GB	GL
TSR H17-24a	25.49	90.82
TSR D18-81	27.15	87.31
TSR D18-52	20.53	86.61
TSR E17-8a	25.27	81.83
TSR C16-21	27.76	89.53
TSR D18-34	26.66	89.99

Table 13. Measurement of the cuboschaphoids of Cervus *sp. nov. from TSR. GB: Greatest breadth.*

Cuboscaphoids	GB
TSR H17-24b	32.65
TSR E17-8c	30.34
TSR D18-102	33.90
TSR D18-53	30.16
TSR C18-13	33.70
TSR C18-9b	33.91
TSR C17-39a	30.90
TSR C17-24	33.98

Table 14. Measurements of the metatarsals of Cervus *sp. nov. from TSR. Fragmented material is noted with (-). The specimen of the young individual is not included.*

Metatarsals	PAP (DAP prox.)	PML (DT prox.)	MML (DT diaph.)	MLEN	FLEN	MAP (DAP diaph.)	AVML	DDML	IDML (DT dist.)	PVML
TSR C18-9a	29.60	29.05	17.92	233.41	227.57	27.21	18.10	31.77	31.82	18.28
TSR H17-24c	30.90	28.00	21.45	239.8	232.15	17.41	18.08	31.20	31.16	17.93
TSR D18-101	33.30	29.94	19.24	238.36	231.26	22.68	18.39	32.91	32.21	18.53
TSR C18-10	34.31	30.96	16.88	241.62	236.71	17.64	18.49	32.84	32.62	18.09
TSR D18-54	29.80	26.58	17.49	227.16	221.13	20.59	17.83	29.27	31.37	18.37
TSR-168	32.03	29.15	-	-	-	-	-	-	-	-

Table 15. Measurements of the proximal phalanges of Cervus *sp. nov. from TSR. L: maximum length, DT: maximum transversal diameter and DAP: maximum antero-posterior diameter.*

Phalanges I	L	DT diaph.	DAP diaph.	DT prox.	DAP prox.	DT dist.	DAP dist.
TSR D18-102	50.59	13.17	16.74	17.73	21.72	14.41	13.86
TSR D18-55	47.91	10.64	15.73	16.16	20.69	12.88	13.47
TSR-194	42.13	10.50	13.76	14.73	16,72	12.47	11.98
TSR D18-110	48.14	11.90	15.98	16.90	20.76	13.90	13.65
TSR D17-40	49.61	12.27	16.94	17.44	21.66	13.68	14.22
TSR C17-47	45.53	11.64	14.54	16.09	19.43	13.68	14.12
TSR-140	48.51	11.41	15.27	15.46	20.75	13.00	13.46
TSR-5	47.07	12.03	15.58	15.11	20.69	13.21	13.19
TSR-14	46.63	11.22	15.23	14.90	21.22	13.50	12.07
TSR C17-39b	51.12	11.72	16.86	17.19	21.13	14.30	13.59
TSR D18-115	45.19	11.74	15.14	15.81	19.51	12.92	13.41
TSR-100	50.12	12.06	16.45	16.59	21.70	14.31	13.85
TSR-143	49.57	11.51	15.93	16.37	21.51	14.60	13.54
TSR D18-97	45.85	11.60	16.13	`16.23	20.67	13.93	14.14
TSR H17-22b	42.24	10.52	13.89	14.12	17.07	11.99	11.48
TSR C18-10	48.43	12.30	16.64	17.42	20.41	13.67	14.06

Table 16. Measurements of the medial phalanges of Cervus *sp. nov from TSR. L: maximum length, DT: maximum transversal diameter and DAP: maximum antero-posterior diameter.*

Phalanges II	L	DT diaph.	DAP diaph.	DT prox.	DAP prox.	DT dist.	DAP dist.
TSR D18-56	33.42	11.53	14.73	15.43	21.21	11.55	15.97
TSR-100	34.66	12.01	14.87	15.96	21.60	12.49	16.51
TSR C18-20	32.50	11.01	14.85	14.90	20.01	11.97	15.82
TSR-143	35.32	11.58	14.50	15.20	20.98	12.75	16.74
TSR H17-22a	29.02	9.71	12.44	13.35	17.00	11.29	15.40
TSR H17-102	35.02	12.35	17.47	16.36	21.14	13.04	16.84
TSR C18-10	35.44	12.42	16.09	16.16	21.53	12.77	16.43
TSR D18-102	36.46	12.22	15.13	16.07	20.53	13.10	16.40

Table 17. Measurements of the distal phalanges of Cervus *sp. nov. from TSR. H: Total height of the articular surfaces (anteroposterior), Ld: length of the dorsal surface/ridge, Lv: length of the palmar surface, B: breadth of the articular surface (transversal).*

Phalanges III	H	Ld	Lv	Breadth
TSR G17-34	18.70	26.37	30.55	11.17
TSR C6-12	22.89	31.42	32.41	15.08
TSR G17-33	18.60	26.67	29.93	11.46
TSR-111	18.97	26.02	30.37	11.20
TSR D18-35	22.07	32.13	32.55	13.49
TSR C16-12	22.78	32.35	31.29	11.67
TSR D18-102	23.32	30. 97	31. 44	14.68
TSR-143	20.29	27.97	31.13	11.93
TSR C18-10	21.92	31.10	31.17	14.12

Table 18. Measurements of the upper dentition of Praemegaceros *sp. from TSR. L: Total length, B: Total breadth.*

Specimen	LM2	BM2	LM1	BM1	LdP4	BdP4
TSR E19-17	31.28	28.41	29.37	25.97	26.24	24.88

Table 19. Measurements of the tibia of Praemegaceros *sp. from TSR. DT: maximum transversal diameter and DAP: maximum antero-posterior diameter.*

Tibia	DT Distal	DAP Distal
TSR H23-2	74.09	53.73

Table 20. Measurements of the astragalus of Praemegaceros *sp. from TSR. DT: maximum transversal diameter, DAP: maximum antero-posterior diameter, L ext: length of the external side, L int: length of the internal side.*

Astragalus	DT diaph.	DAP diaph.	DT prox.	DAP prox.	DT dist.	DAP dist.	L ext.	L int.
TSR D13-12	40.95	35.17	37.81	31.32	43.51	31.08	61.06	57.22

Table 21. Measurements of the proximal phalanges of Praemegaceros *sp. from TSR. L: maximum length, DT: maximum transversal diameter and DAP: maximum antero-posterior diameter.*

Phalanges I	L	DT diaph.	DAP diaph.	DT prox.	DAP prox.	DT dist.	DAP dist.
TSR D23-4	66.45	25.70	24.86	29.55	32.72	26.68	23.42
TSR H18-7	67.45	23.79	25.20	28.17	32.57	25.60	22.58

Table 22. Measurements of the medial phalanx of Praemegaceros *sp. from TSR. L: maximum length, DT: maximum transversal diameter and DAP: maximum antero-posterior diameter.*

Phalanx II	L	DT diaph.	DAP diaph.	DT prox.	DAP prox.	DT dist.	DAP dist.
TSR-125	45.86	21.63	23.83	27.74	34.47	23.40	32.95

Table 23. Measurements of the distal phalanges of Praemegaceros *sp. from TSR. H: Total height of the articular surfaces (anteroposterior), Ld: length of the dorsal surface/ridge, Lv: length of the palmar surface, B: breadth of the articular surface (transversal).*

Phalanges III	H	Ld	Lv	Breadth
TSR D18-36	38.93	45.90	57.9	20.95
TSR-37	34.68	40.27	52.14	18.72

Appendix II

Plate I. *Cervus* sp. nov.

Antlers

(1) Second tine, dex (TSR D17-41)
    i. Internal view
    ii. External view
(2) Antler beam, young individual (TSR-167)
(3) Antler, dex (TSR D18-100)
    i. External view
    ii. Internal view
(4) Antler, sin (TSR D18-100)
    i. External view
    ii. Internal view
(5) Antlers (TSR D18-100)
    i. Frontal view, dex
    ii. Frontal view, sin
(6) Antlers (sin and dex), frontal view

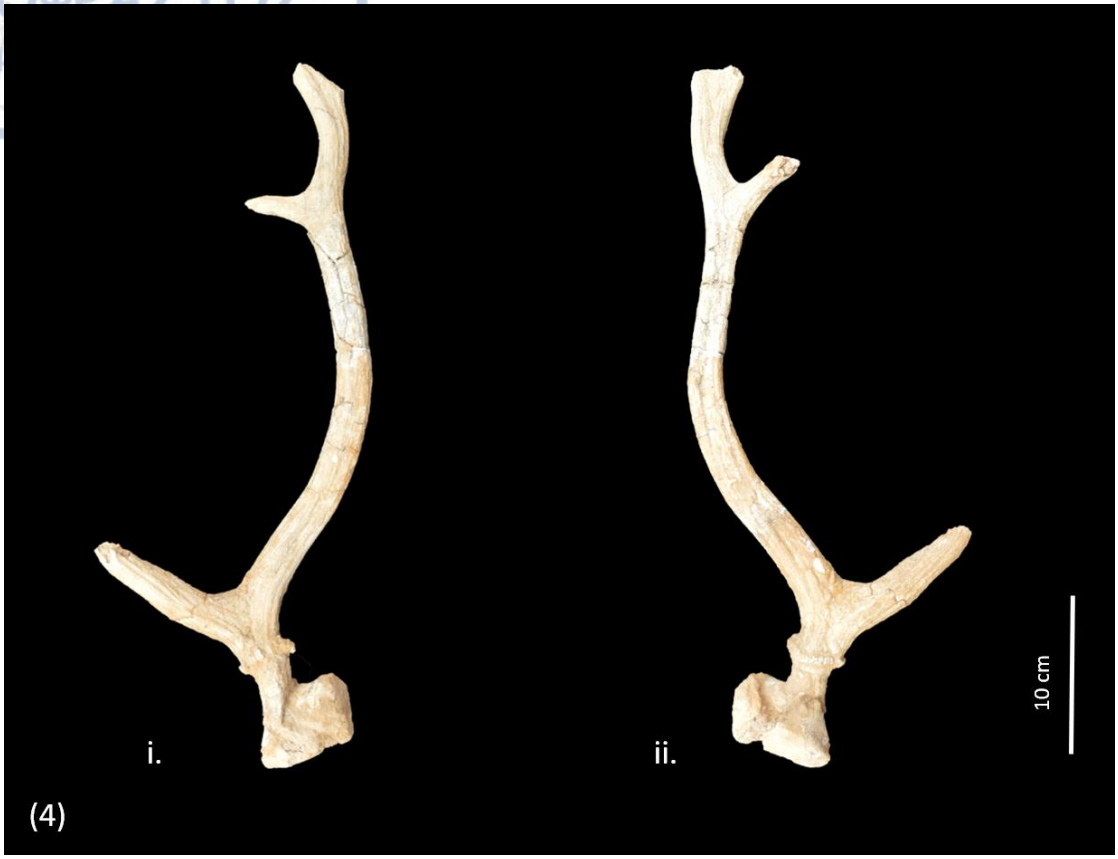

(4)

(5)

Plate II. *Cervus* sp. nov.

(7) Maxillae – occlusal view

i. P2-M3, sin (TSR-156)

ii. P2-M3, sin (TSR-135)

iii. dP2-M1, dex (TSR G16-38)

(8) Mandibular fragments – occlusal view

i. p3-m2, sin (TSR E13-5)

ii. p2-m2, dex (TSR F20-49)

(9) Complete mandible – occlusal view: p2-m3, dex (TSR D18-99)

(10) Complete mandible – lateral view: p2-m3, dex (TSR D18-99)

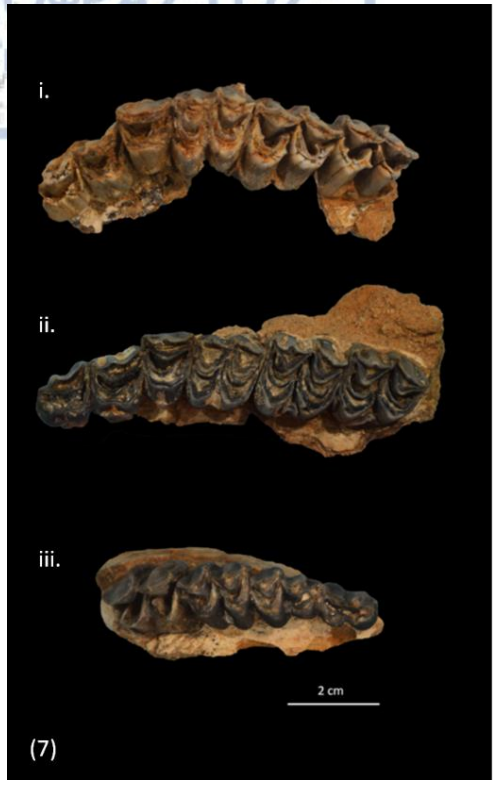

Plate III. *Cervus* sp. nov.

(1) Front leg

i. Humerus, sin (TSR-149) – anterior view

ii. Radius dex, young individual (TSR H17-22d) – posterior view

iii. Radius dex, young individual (TSR H17-22d) – anterior view

iv. Metacarpal dex, young individual (H17-22c) – dorsal view

Plate IV. *Cervus* sp. nov.

Hind leg

(1) i. Femur sin (TSR D18-48) – posterior view; ii. Tibia, sin (TSR D18-50) – posterior view

(2) i. Calcanei – medial view; ii. Astragali – dorsal view; iii. Cuboscaphoids – proximal view; iv. Cuboscaphoids – distal view

(3) i. Proximal epiphyses of metatarsals; ii. Metatarsals – dorsal view

(4) Articulated metatarsal and phalanges – anterior view

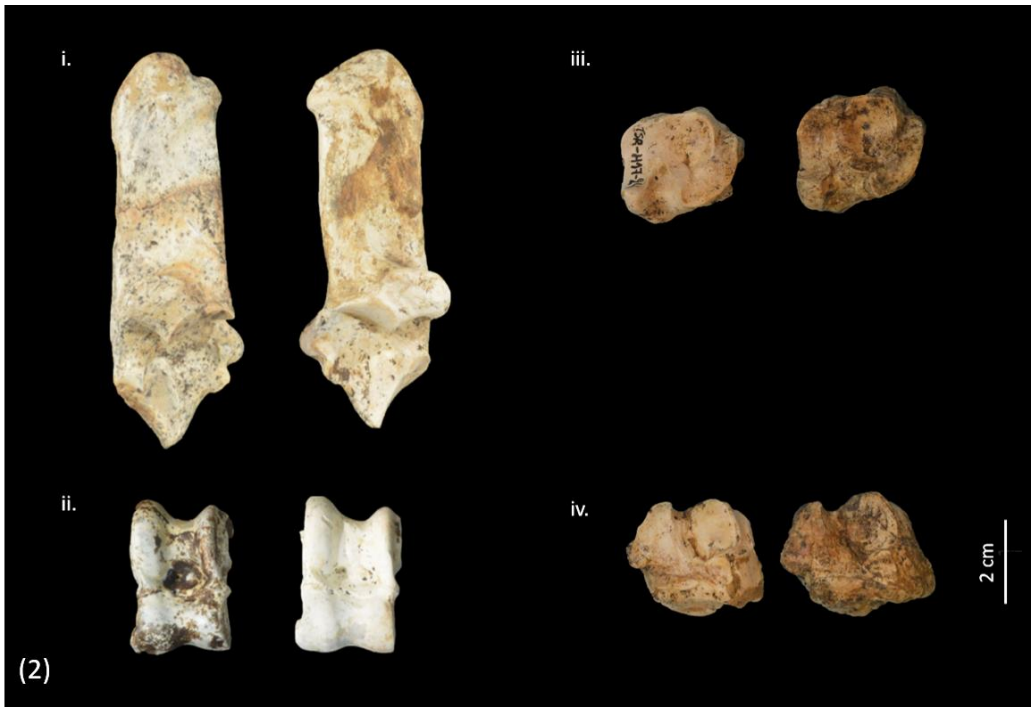

Plate V. *Praemegaceros* sp.

(1) Maxilla – occlusal view: dP3-M2, dex (TSR E19-17)

(2) Tibia dex (TSR H23-2)

i. Dorsal view

ii. Distal epiphysis

(3) Astragalus sin (TSR D13-12)

i. Dorsal view

ii. Lateral view

(4) Phalanges

i. Phalanges I (TSR H18-7, TSR D23-4)

ii. Phalanx II (TSR-125)

iii. Phalanges III (TSR D18-36, TSR-37)